Title: Study on sulfur deactivation of catalysts for DMDS oxidation

Authors: Bouchra Darif, Satu Ojala, Marja Kärkkäinen, Stéphane Pronier, Teuvo Maunula, Rachid Brahmi, Riitta L. Keiski

PII: S0926-3373(17)30070-X
DOI: http://dx.doi.org/doi:10.1016/j.apcatb.2017.01.053
Reference: APCATB 15366

To appear in: *Applied Catalysis B: Environmental*

Received date: 5-9-2016
Revised date: 18-1-2017
Accepted date: 22-1-2017

Please cite this article as: Bouchra Darif, Satu Ojala, Marja Kärkkäinen, Stéphane Pronier, Teuvo Maunula, Rachid Brahmi, Riitta L.Keiski, Study on sulfur deactivation of catalysts for DMDS oxidation, Applied Catalysis B, Environmental http://dx.doi.org/10.1016/j.apcatb.2017.01.053

Study on sulfur deactivation of catalysts for DMDS oxidation

Bouchra Darif[1,2], Satu Ojala[1], Marja Kärkkäinen[1], Stéphane Pronier [3], Teuvo Maunula[4], Rachid Brahmi[2]* and Riitta L. Keiski[1]

1-Environmental and Chemical Engineering (ECE), Faculty of Technology, P.O. Box 4300, FI-90014 University of Oulu, Finland.
2-Laboratory of Catalysis and Corrosion of Materials (LCCM), Department of Chemistry, Faculty of Sciences of El Jadida, University of Chouaib Doukkali, BP.20, 24000 El Jadida, Morocco.
3- Institute of Chemistry of Poitiers: Materials and natural resources (IC2MP), CNRS-UMR 7285, University of Poitiers B27, Rue Michel Brunet, 86073 Poitiers cedex 9 France.
4- Innovations and R&D, Catalyst Development, Dinex Ecocat Oy, 41330 Vihtavuori, Finland.

∗ Corresponding author: rachid.brahmi@univ-poitiers.fr

Graphical abstract

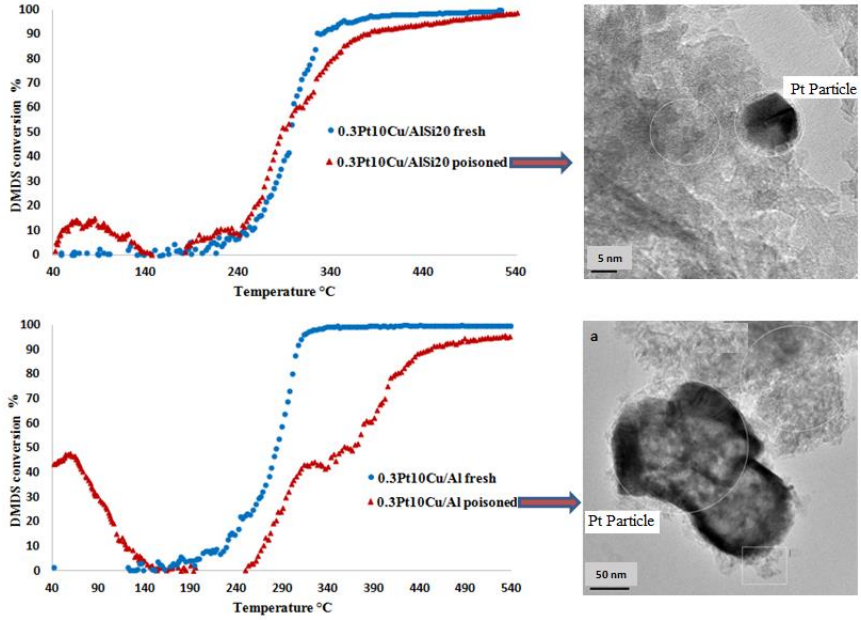

Highlights:

1- 0.3Pt10Cu/$AlSi_{20}$ catalyst is active, selective and durable in DMDS oxidation
2- Less than 20% of silica is able to improve catalyst resistance against sulfur
3- PtO is the most optimal form of platinum in Pt-Cu catalyst for DMDS oxidation

Abstract

In the present research, an industrially aged Pt/Al_2O_3 catalyst was used as a basis for the study on the sulfur deactivation and the development of more resistant catalytic materials. The catalytic activities of both industrially and laboratory-aged materials in DMDS oxidation were studied in addition to characterization by XRD, XPS, FESEM, TEM and N_2 adsorption. The industrial ageing induced a phase change from γ-Al_2O_3 towards θ-Al_2O_3, formation of aluminum sulfates and an increase in Pt particle size as well as a change in the oxidation state of Pt to a higher state. These changes caused an increase of 30°C in the light-off temperature for DMDS oxidation. Accelerated ageing in the presence of SO_2 and H_2O vapor at 400°C for 5 h decreased the activity of the Pt/Al_2O_3 at the same level than for the industrially aged catalyst even though smaller sulfur content and no sintering of γ-Al_2O_3 were observed. Pt sintering (10-20 nm) in both cases was observed. The XPS results confirmed the formation of new sulfate phases and the interaction between sulfur and the active phase as well as the support of the catalyst undergone accelerated ageing. After the

accelerated ageing of copper-based catalysts, the $0.3Pt10Cu/Al_2O_3|_{0.8}SiO_2|_{0.2}$ catalyst showed an interesting resistance towards sulfur deactivation, as it was expected.

Keywords: Dimethyldisulfide, Pt-Cu catalysts, sulfur deactivation, accelerated ageing, industrial ageing, SVOC oxidation and sulfur tolerance.

1. Introduction

Sulfur containing volatile organic compound (SVOC) emissions are released mainly from gasoline combustion, evaporation of liquid fuels and solvents, from oil and gas refineries and pulp and paper industry. The increasing environmental concern and difficult management of these compounds have contributed to a growth in the number of large-scale industrial disposal operations in the developing countries [1]. Dimethyldisulfide ($C_2H_6S_2$, DMDS) is among the most odorous compounds due to its low human detection threshold (2.5 μgm^{-3}), which makes it rather difficult to treat completely [2]. The catalytic oxidation is the most attractive way to remove VOCs at low concentrations from industrial gaseous effluents [3], and it has shown to be a potential method also in the case of SVOCs[4].

The catalysts that are commonly used for VOC oxidation are supported precious metals, metal oxides and mixed metal oxide-precious metal catalysts [5-8]. Precious metals have higher activity compared to metal oxides, however, they are susceptible to poisoning and expensive [9]. Mixed metal oxides represent one of the most important and widely employed classes of solid catalysts, either used as an active phase or as a support. Oxides of transition metals, mainly Mn [10-13], Co [9, 14-16], Fe [10] and Cu [13, 17] are employed for the oxidation of VOC. However, these catalysts are frequently deactivated due to the sulfur poisoning [18]. Sulfur compounds bond tightly to the active site of the catalyst forming stable surface metal sulfides, which prevent adsorption of reactants on the surface [19]. Sulfur can also concentrate on the oxide support forming sulfates (e.g. aluminum sulfates and cerium oxy-sulfates), which can have an impact on the metal-support interaction [19, 20].

This present study will shed a light on the catalytic oxidation of SVOCs. The model compound used in this study is DMDS, which is known to be present in high concentrations in industrial exhaust gases. The catalysts applied to the destruction of SVOCs must be highly active at relatively low temperatures and maintain high resistance towards deactivation by sulfur and its derivatives

compounds as well as have high selectivity towards CO_2 and SO_2. For these reasons, the major aims of this study are the following:

1- to characterize and study the activity of the industrially aged 1wt%Pt/Al_2O_3 catalyst (in powder form);
2- to develop a representative laboratory ageing procedure to mimic the real-life deactivation of an SVOC catalyst, using the results from the industrially aged 1wt%Pt/Al_2O_3 catalyst;
3- to study the deactivation of the laboratory made catalysts by developed accelerated ageing protocol, i.e. 0.3Pt10Cu/Al and 0.3Pt10Cu/$AlSi_{20}$. These catalysts were chosen, because they had shown resistance against sulfur poisoning in our earlier study [21].

2. Experimental

2.1 Catalyst preparation

Three different catalysts were studied in this work. The 1wt-%Pt/Al_2O_3 catalyst was supplied by Dinex Ecocat Oy Company, (the catalyst later denoted as Pt/Al) and two other catalysts, 0.3Pt10Cu/Al and 0.3Pt10Cu/$AlSi_{20}$, were prepared in the laboratory. The Pt/Al catalyst was used in the industrial ageing and in the development of the accelerated ageing protocol. The laboratory-made catalysts were developed with an aim to improve the catalyst stability. The durabilities of these catalysts were studied with accelerated ageing. The preparation of the boehmite gel was done based on the procedure described by Yoldas [22] after small modifications. A known mass of aluminum tri-sec-butoxide ($Al[OC_4H_9)_3]$, 97%, Alfa Aesar) was mixed with ultrapure water corresponding to the molar ratio of $n(H_2O)/n(Al) = 100$. The mixture was homogenized under stirring at 60 °C for 1 h. Then, two drops of hydrochloric acid (HCl) were added to catalyze the peptization reaction. For doped alumina (80 mol-%Al_2O_3-20 mol-%SiO_2), tetraethoxysilane ($Si(OC_2H_5)_4$, 99%, Aldrich), was introduced simultaneously with HCl acid. Then the mixture was heated at 80 °C for 2 h. During the synthesis, the reaction mixture was stirred and the beaker was covered with a watch-glass to minimize evaporation of water. Under these synthesis conditions (excess water, acid and temperature of 80 °C), the hydrated boehmite doped silica (AlO(OH)-$SiO_2 \cdot nH_2O$) was formed. The whitish gel obtained, was then dried at 120 °C overnight, and then grounded, leading to the formation of a white powder of boehmite-type doped xerogel. After that, the powder was calcined from RT to 550 °C for 5 hours with a temperature rise of 5 °C min^{-1}.

The co-impregnation method was used to prepare the bimetallic Pt-Cu catalysts supported separately on the materials mentioned above with 0.3 wt-% platinum and 10 wt-% copper loadings. The preparation was done using chloroplatinic acid hexahydrate ($H_2PtCl_6 \cdot 6H_2O$, 99,9%, Alfa Aesar) and copper(II) nitrate hemipentahydrate ($Cu(NO_3)_2 \cdot 2.5H_2O$, 98%, Alfa Aesar) as active phase precursors. After dissolving the precursors with ultrapure water and introducing the support material, mechanical stirring was continued at room temperature overnight. Then the sample was dried at 65 °C using a sand-bath. Finally, the catalyst samples, 0.3Pt10Cu/Al and 0.3Pt10Cu/$AlSi_{20}$, were calcined in air at 550 °C for 5 h.

2.1 Characterization

The final loading of platinum and copper, and the total sulfur contents of the catalysts were analyzed using X-ray fluorescence spectroscopy (XRF). The measurements were performed using PANalytical Axios instrument. The supports and catalysts were also characterized by physisorption of N_2 at -196 °C performed with Micrometrics ASAP2020 to find out the specific surface area and the porosity. Identification of phases was done by X-ray diffraction (XRD) measurements. The XRD data were collected at room temperature, using a Siemens D5000 diffractometer equipped with a Cu anode (λ_{Cu} = 1.5418 Å) and a nickel filter. Additional acquisition parameters were: 2θ range 5-90 °; step 0.025 ° and dwell time of 1 s. Diffraction patterns were compared to the ICDD database (International Center for Diffraction Data) for the identification of crystalline phases.

A Zeiss Ultra Plus field emission scanning electron microscope (FESEM) equipped with an energy-dispersive X-ray spectroscopy (EDS) at an accelerating voltage of 15.0 kV was used to study the surface of the Pt/Al, 0.3Pt10Cu/Al and 0.3Pt10Cu/$AlSi_{20}$ catalysts before and after the ageing procedures.

In order to obtain quantitative measures of particle and/or grain size, size distribution, and morphology, Transmission Electron Microscopy (TEM) was performed using a JEM-2100 LaB_6 equipped with energy dispersive spectrometer EDS.

The X-ray photoelectron spectroscopy (XPS) analyses of Pt/Al, 0.3Pt10Cu/Al and 0.3Pt10Cu/$AlSi_{20}$ were performed with a Thermo Fisher Scientific ESCALAB 250Xi XPS equipped with the Al K_α X-ray source =1486.7 eV to study the oxidation states of copper and platinum elements. The X-ray source operated at 10 mA and 12 kV. The spectral regions corresponding to Cu 2p, Pt 4d, Pt4f, Al 2p, S 2p and O 1s core levels were recorded for each

sample. The static charge of the samples was corrected by referencing all binding energies (BE) to the Al 2p peak (BE= 72.6 eV) and Shirley function was used as a background.

2.2 Catalyst testing

The activities of the catalysts were tested in the total oxidation of dimethyldisulfide CH_3-S_2-CH_3 (DMDS) with the concentration of 550 ppm in 1 L.min^{-1} of purified air at the temperature range from room temperature to 600 °C with the heating rate of 5 °C.min^{-1}. The Gas Hourly Space Velocity (GHSV) was fixed at 76 500 h^{-1}. 100 mg of the catalyst sample was placed between two layers of quartz sand, 100 mg of each, and then packed into a tubular reactor with quartz wool plugs. The gas composition was measured with an FTIR (Gasmet, Model Cr2000) already descried in previous work [21].

The conversion of DMDS is defined in the following way:

$$\text{Conversion } (\%) = \frac{Ci - Co}{Ci} \times 100 \quad (1)$$

where C_i is the initial feed concentration of dimethyldisulfide DMDS (ppm), C_0 is the outlet concentration of DMDS (ppm).

2.3 Accelarated deactivation procedure

In order to speed up the deactivation and to create a representative way how to simulate the industrial ageing of the catalysts, three catalyst samples were exposed to a specific treatment. The accelerated deactivation was carried out in the gas phase using a flow reactor. The powder form sample was placed in a vertically positioned tubular quartz reactor between layers of quartz wool. The mass of the sample was 100mg.

The treatment was conducted under the following conditions: 100 ppm SO_2, 10 vol-% of H_2O, and 10 vol-% of air, balanced with N_2. The furnace was heated from room temperature to 400 °C under a flow of nitrogen and air with a heating rate of 10 °C min^{-1}. Once reaching the target temperature (400 °C), SO_2 and H_2O were added into the gas mixture. After 5 h of treatment, the furnace was cooled down to the room temperature under a nitrogen and air flow.

The terms used later to describe the studied catalyst type in this article are the following:
Fresh catalyst: Catalyst which has not undergone any type of aging;
Used catalyst: Catalyst which has undergone an industrial aging;
Poisoned catalyst: Catalyst that has been aged with the accelerated ageing procedure.

2.4 Industrial ageing of the catalysts

The ageing of the catalysts in industrial conditions was done during pilot experiments at Stora Enso Oulu paper mill in 2005-2006. During the pilot experiments, about 10 % of the chip bin emissions were treated in a catalytic incinerator with a capacity of 500 $m^3.h^{-1}$. The industrial emissions consist roughly about 40 % of terpenic compounds and 60 % reduced sulfur compounds by volume. The identified compounds from the emission stream were methanol, terpenic compounds, hydrogen sulfide, dimethyl sulfide, dimethyl disulfide and methyl mercaptane. In addition, the emission contained a significant amount of moisture, and solids (content about 0.003 $kg.h^{-1}$) the amounts of which were reduced by condensation and filtration before the catalytic incinerator. [23] The test catalysts were placed inside a custom-made ageing rack [24], which was placed inside the regenerative catalytic incinerator between the heat exchanger and the catalyst. In this way, depending on the periodical operation of the incinerator, the catalysts were exposed to both the unreacted emission stream and the treated emission stream (reaction products). Through the ageing, the temperature of the incinerator close to the ageing rack was varying between 330-530°C. During the downtimes, the incinerator was cooled down close to the outdoor temperature, which was at minimum -20 °C, since the pilot experiments were done during the wintertime. The total duration of the industrial ageing was about 2 months, of which the exact uptime was 1355 hours giving a utilization rate of about 88.5% for the incinerator.

3. Results and discussion

3.1 Activity and characterization of the fresh and industrially aged catalysts

To study the performance of the Pt/Al catalyst, and to compare its activity after the industrial ageing, catalytic activity tests have been carried out in the total oxidation of DMDS. The conversion of DMDS over the Pt/Al catalysts is shown in Figure 1. The results indicate that the two months industrial ageing decreased the activity of the Pt/Al catalyst.

Figure 1. Light-off tests of DMDS oxidation over fresh and used Pt/Al catalysts.

The fresh Pt/Al catalyst seems to be relatively active in the catalytic oxidation of DMDS at high temperatures (T_{90} = 425 °C) according to Figure 1 and Table 1. In the case of the used catalyst, it was noticed that the catalytic performance in DMDS oxidation decreases by 29 °C in terms of both T_{50} and T_{90}. This result shows that the active surface of the catalyst has been modified and/or the formation of new phases on the surface of the studied catalyst has taken place, which prevents the catalyst to work as efficiently as the fresh one.

To study the assumption mentioned above in detail, different characterization methods such as XRF, XRD, BET, FESEM, TEM-EDX and XPS were used.

The fresh and used Pt/Al catalysts showed almost the same shapes of nitrogen adsorption-desorption isotherms and according to the International Union of Pure and Applied Chemistry (IUPAC), they correspond to the isotherms Type IV [25-28]. Both the catalysts showed also the same type of hysteresis, Type H2. This hysteresis observed confirms the presence of tubular pores open at both ends and a good inter-connectivity of the pores [29-30]. It was noted also that the desorption is slower on the used catalyst, which is probably due to the new species formed on the surface that could retain N_2 molecules.

The specific surface areas of the catalytic materials and their pore volumes are presented in Table 2.

It can be observed from Table 2 that the surface area of the used Pt/Al catalyst has decreased severely in comparison to the fresh catalyst. This reduction in the BET surface area could have been caused by a sintering phenomenon due to the crystal growth on the surface of the used catalyst. This change in the structure of the used Pt/Al catalyst may be a physical process where the active surface of the catalyst decreases by structural changes induced by e.g. temperature [31, 32]. Typically, thermal deactivation occurs when the temperature rises unexpectedly to high values, causing both sintering of the precious metals and catalytic supports [33, 34]. In the case of Al_2O_3 support, sintering occurs during the phase transformation, whilst γ-alumina is gradually transformed into θ-alumina at high temperatures, resulting in a loss of the surface area. It was found that dispersed metals in supported metal catalysts can also accelerate support sintering [35-39]. Furthermore, thermal deactivation can cause more severe changes in presence of H_2O [40].

Figure 2. XRD patterns of the catalysts (a) fresh Pt/Al and (b) used Pt/Al.

In the case of used Pt/Al_2O_3, an apparition of new phase was observed. According to the X-ray diffraction results presented in Figure 2, sintering has occurred due to the phase transformation, when γ-alumina (ICDD: 00l-050-0741) has transformed into θ-alumina (ICDD: 00-023-1009), resulting in a loss of the surface area. Normally, the formation of θ-alumina appears at around 1000 °C [41], which is not probable in the industrial ageing conditions due to safety reasons. However, the presence of impurities and considerable amount of moisture alters the barrier of phase transformations. For example, calcination of γ-Al_2O_3 with 3 wt-% platinum impurity can lead to the formation of α-Al_2O_3 below 1100 °C [42-44] and the water existence can encourage also early sintering and formation of the stable α-alumina [45].

Another result found by the XRD analysis is related to the existence of new compounds formed on the catalysts used, namely aluminum sulfate that can be explained by the non-selective poisoning when sulfur (coming from the feed gas or being reaction by-products) is deposited on the alumina support by forming new compounds and masking the pores. This may partly explain also the loss of the specific surface area observed based on the BET measurements. The formation of aluminum sulfate is a type of chemical deactivation. The chemical deactivation may be considered as a poisoning process where the catalytic oxidation performance decreases due to the chemisorption of undesirable elements on the active metal and the catalyst support [32, 46]. The poisoning species such as sulfur (S) may exist in the reactants and the reaction products in the form of organic or inorganic compounds. It was reported that the formation of $Al_2(SO_4)_3$ on the surface of Pt/Al_2O_3 (if SO_2 or sulfur compounds exist in the gas feeding) could block catalyst pores and lower its oxidation activity [47-49]. XRF analysis highlights a bulk sulfur concentration about 17% in the used Pt/Al catalyst. Due to the low content of Pt, the conclusions regarding the deactivation of active metal by sulfur were not possible by XRD.

Concerning the noble metals and especially Pt, sintering may occur at rather low temperature (about 600 °C) [34]. The effect of temperature on sintering of metals and oxides can be understood physically in terms of the driving forces for dissociation and diffusion of surface atoms, which are both proportional to the fractional approach to the absolute melting point temperature (T_{mp}). Thus, as temperature increases, the mean lattice vibration of surface atoms increases. When the Hüttig temperature ($0.3T_{mp}$) is reached, less strongly bound surface atoms at defect sites (e.g., edges and corner sites) dissociate and diffuse readily over the surface, while at the Tamman temperature ($0.5T_{mp}$), atoms in the bulk become mobile. Accordingly, sintering rates of a metal or metal oxide

are significant above the Hüttig temperature and very high near the Tamman temperature. Thus, the relative thermal stability of metals or metal oxides can be correlated in terms of the Hüttig or Tamman temperatures [50]. Table 3 gives data of T_{Tamman} and $T_{Hüttig}$ for selected metals and their oxides. The melting point is not always well-defined, for instance some oxides already begin to decompose before T_{Tamman} or $T_{Hüttig}$ has been reached.

The measured temperatures during the industrial ageing have been in maximum 530°C, however, the catalyst surface may have reached much higher temperatures before the emergency shutdown of the pilot incinerator. The temperature measurement in the incinerator was made with a PT100 sensor about ~20 cm away from the catalyst ageing rack. We can estimate that the $T_{Hüttig}$ temperature for Pt and Al_2O_3 have been passed during the ageing. In addition, the T_{Tamman} for PtO and PtO_2 have been reached easily. In conclusion, the precious metals have probably coagulated to larger particles resulting in a lower active surface area. To verify that assumption, TEM analyses were made to reveal information on the internal structure of fresh and used Pt/Al catalysts, including the characterization of Pt particle architecture and the assessment of their sizes.

Figure 3. TEM images of a) fresh Pt/Al and b) used Pt/Al.

For fresh Pt/Al catalysts (Figure 3.a), the TEM results showed that Pt particles seem to be fairly uniform in size, in the order of 7 nm, and relatively well dispersed. Concerning the used Pt/Al catalyst (Figure 3.b), the Pt particles were found not to be homogeneously uniform on the surface of the catalysts and some of the Pt particles were sintered and measured to be about 10 nm. Moreover, the TEM coupled with an EDX analysis showed that sulfur is deposited not only on the support, but also on the active phase, i.e. Pt, as Figure 4 and Table 4 show.

Figure 4. TEM image of used Pt/Al catalyst used for EDS analysis

To get an overview about the sulfur deposition on the Pt/Al, FESEM images with elemental mapping were made. Figure 5 shows that some overlapping of S, O and Al exist. This confirms the fact that new compounds such as aluminum sulfate has been formed on the surface of the support.

Figure 5. Elemental mapping by FESEM for O, Al and S species on the surface of the used Pt/Al catalyst.

The XPS spectra of fresh and used Pt/Al catalysts were evaluated in order to identify and compare the oxidation state of the active species on the surface, to explain in more detail how and why Pt/Al was subjected to a deactivation. The decomposition spectra of individual components of Pt $4d_{5/2}$ level, showed the presence of only one kind of platinum in the case of the fresh Pt/Al catalyst (Figure 6.a). The spectral peak ($Pt4d_{5/2}$) with BE at around 315.8 eV is associated with Pt (0).

For the used Pt/Al catalyst, the decomposition spectra of individual components of Pt baseline $4d_{5/2}$ showed the presence of two platinum species (Figure 6.b). According to literature, the spectral peak ($Pt4d_{5/2}$) of BE at around 315 eV is associated with the chemical state of Pt(0), but the last peak at 318.5 eV corresponds either to Pt(IV) or to the platinum species interacting with the ionic SO_4^{2-} of the metallic interface of the support [49]. Due to low concentration of the Pt species on the sample surface, the XPS spectra for Pt $4d_{5/2}$ contain considerable amount of noise that may affect the evaluation of the results. However, the differences between the fresh and the used Pt/Al catalysts are visible.

Figure 6. Decomposition of Pt $4d_{5/2}$ component of a) fresh Pt/Al and b) used Pt/Al.

The spectral decomposition of individual components of O1s level showed the presence of three oxygen species in the case of the fresh Pt/Al catalyst (Figure 7.a). Both spectral peaks (O1s) with BE at around 530 and 531 eV are associated with the oxygen atoms in the oxide network and the last peak at 532 ± 0.3 eV is coming from the surface oxygen such as hydroxyl groups [51]. For the used Pt/Al catalyst, the results showed the presence of two oxygen species (Figure7.b). The spectral peak (O 1s) with BE at around 530.5 eV is associated with the oxygen atoms in the oxide network and the last peak at 532.4 eV could be derived from oxygen in the sulfated groups of $Al_2(SO_4)_3$.

Figure 7. Decomposition of O1s component of a) fresh Pt/Al and b) used Pt/Al.

For S species, and according to the decomposition of the individual components of spectral levels S 2p (Figure 8), the binding energy of the $S2p_{1/2}$ = 168.8 eV and S $2p_{3/2}$ = 167.5 eV showed that sulfur

is present only in the form of S^{6+} [52-55]. Thus, it can be deduced that sulfur is present in a single form and a single type of sulfate on the surface structure of the catalysts, as shown by the presence of a single transition $S2p_{1/2}$ and of $S2p_{3/2}$.

Figure 8. Decomposition of S2p component of used Pt/Al catalyst.

Table 5 shows the atomic ratios observed on the surface of the studied catalysts determined by XPS. In the case of the used catalyst, it was found that the Al amount on the surface decreased, which may be explained by either a possible formation of a new compound or that the Al species were covered by other species. Concerning Pt, it was found that its concentration remained about the same. Because the surface concentration of Pt remained the same between the fresh and the used catalyst while the aluminum content decreased, we could conclude that most of the sulfur poisoning appears on the alumina support, but this assumption should be ruled out since TEM-EDS showed that sulfur appears on the active phase, too.

To summarize the results of the industrial ageing, the decrease of the catalytic activity of Pt/Al catalyst by DMDS oxidation experiments was first observed. With different characterization techniques, changes in catalyst physico-chemical properties were detected. Those were a significant decrease in specific surface area, sintering of Pt species and appearance of Pt(IV) species that are less tolerant to sulfur as well as appearance of sulfur-compounds both on the active phase and the support. In the next step of the research, the aim was to develop an accelerated ageing protocol representing the industrial ageing.

3.2 Development of accelerated ageing protocol

In order to simulate the industrial deactivation of the catalysts by sulfur, an accelerated ageing procedure was developed based on the information from the industrially aged Pt/Al catalyst. The validation of the accelerated ageing procedure was done with the fresh Pt/Al catalyst. The Pt/Al catalyst undergone the accelerated ageing is later called as the poisoned Pt/Al. Figure 9 presents the comparison of the catalytic activity between the fresh, used and poisoned Pt/Al catalysts.

Figure 9. Light-off tests for DMDS oxidation over fresh, used and poisoned Pt/Al catalysts.

The results in Figure 9 and Table 6 show that the accelerated ageing decreased the activity of the Pt/Al catalyst in the oxidation of DMDS. The catalytic activity decreased compared to the fresh catalyst, and the light-off curves of used and poisoned Pt/Al were relatively close to each other. Qualitatively, it seems that the accelerated ageing procedure is able to represent the industrial ageing when it lasted just 5 hours.

To elucidate the ageing mechanism, different characterization methods have been used. The specific surface areas and pore information for fresh, used and poisoned catalysts are presented in Table 7.

After conducting the accelerated ageing for Pt/Al, it can be noted that the surface area and total pore volume of the catalyst decreased about 50 %. However, the decrease was not as severe as in the case of the industrially aged catalyst probably due to the aging time that is much longer in the case of industrial test.

In the XRD analysis of the poisoned Pt/Al, no evidence on aluminum sulfate or sulfide was found. This is most probably due to the relatively small total sulfur content (0.9 %) observed by XRF. During the accelerated ageing treatment, temperature was controlled carefully and it was at maximum 400 °C. At this temperature severe thermal deactivation of alumina nor platinum are not expected, and in fact, no other phase than γ-Al_2O_3 was observed in the XRD analysis. However, the $T_{Hüttig}$ for PtO and T_{Tamman} for PtO_2 phases are passed indicating the slight possibility for the increase in the particle size. In order to confirm this, a TEM measurement was done for the Pt/Al poisoned catalyst (Figure 10).

Figure 10. TEM image of poisoned Pt/Al.

Figure 10 shows the TEM image of the poisoned Pt/Al catalyst. Some of the Pt particles seem to be sintered and their size was measured to be around 20 nm, which was assumed to be possible based on Tamman and Hüttig temperatures. This result is an indication of similar sintering occurring

during both industrial and accelerated ageing. According to the EDS measurements (Table 8), sulfur appears on both the active phase and the support.

Sulfur was also observed on the same positions with aluminum and oxygen based on FESEM imaging with elemental mapping presented in Figure 11. Interaction of sulfur with Pt was not possible to observe by FESEM due to the small particle size of Pt.

Figure 11. Elemental mapping by FESEM for Al, O and S species on the surface of the poisoned Pt/Al catalyst.

Both the electron microscopies give indications about the existence of sulfur accumulation on the support, even though not clear evidence by XRD was observed.

The XPS spectra of the poisoned Pt/Al catalyst was analyzed in order to identify and compare the oxidation states of the active species on the surface and to confirm if the accelerated deactivation method gave similar results compared to the industrial ageing. The decomposition spectra of individual components of the Pt $4d_{5/2}$ level of the poisoned Pt/Al catalyst showed the same behavior as in the case of the used Pt/Al catalyst. The spectra showed the presence of two platinum species (Figure 12.a). The spectral peak (Pt $4d_{5/2}$) of BE at around 315 eV is associated with the chemical state of Pt (0), and the last peak at 318.5 eV corresponds either to Pt IV or to the platinum species interacting with the ionic SO_4^{-2}[56].

For O1s, the same chemical composition was found compared to the case of the used Pt/Al catalyst, which is the presence of two oxygen species in both cases (Figure 12.b). The spectral peak (O 1s) with BE at around 530.5 eV is associated with the oxygen atoms in the oxide network and the last peak at 532.4 eV could be derived from oxygen in $Al_2(SO_4)_3$.

According to Figure 12.c, it can be deduced that sulfur is present in a single form and a single type of sulfate S^{6+} [52-55] in the surface structure of the poisoned Pt/Al catalyst, as shown by the presence of a single transition $S2p_{1/2}$ and of $S2p_{3/2}$. Thus, based on the XPS results, it can be concluded that the accelerated aging had affected the surface of the Pt/Al catalyst in the similar way than the industrial ageing in terms of sulfur interaction.

Figure 12. Decomposition of XPS peaks of poisoned Pt/Al: a) Pt, b) O and c) S.

Table 9 shows the results of the catalyst component atomic ratios on the surface of fresh and poisoned Pt/Al catalysts analyzed by XPS. Apparently the Al content is slightly reduced compared to the fresh Pt/Al, which means that sulfur is deposited on the support surface, but in lower amounts than in the case of the used catalyst, that is confirmed by the ratio S/Al = 0.2.

To summarize, according to the BET-BJH data, the surface area of Pt/Al decreased by only 52 % compared to the fresh Pt/Al (95 % decrease for the used catalyst) and yet the catalytic activity decreased. In the case of the industrially aged Pt/Al, the decrease in specific surface area was due to both thermal deactivation and poisoning caused by sulfur. In the case of accelerated ageing, no thermal changes were observed for the support, but some indication of Pt sintering was observed by TEM. Thus, it is expected that the decrease in catalytic activity after accelerated ageing is mainly due to sulfur poisoning, since sulfur was observed to be present on Pt particles and on the support material. According to the XPS results, the presence of Pt (0) and Pt (IV) species was found on the surface of the Pt/Al catalyst, which can provide an environment in which the SO_2 interactions can happen faster [21]. Based on the catalytic activity tests and the structural and textural information obtained by different characterization methods, the accelerated ageing procedure has led to a similar type of catalyst deactivation as the industrial scale ageing, and this has happened especially in a qualitative way, since the sulfur content was smaller than the one in the industrially deactivated catalyst and the loss of the specific surface area was not equal in amount. Based on results, it was agreed that the accelerated ageing was adequate enough, even though, higher temperatures could be used to induce also the thermal deactivation observed in the case of used Pt/Al. Then, the research focus was directed towards studying more sulfur-resistant catalytic materials.

3.3 Sulfur poisoning of bimetallic catalysts

The same reason, which makes the Pt/Al catalyst a good model material for the development of accelerated ageing protocol for the SVOC treatment, makes it a bad selection for the actual industrial treatment process. This is why the last part of the paper is devoted to the studies on the development of better catalytic material with improved activity, selectivity and stability. We have found in our earlier studies that the doping of Al_2O_3 with SiO_2 will improve the catalyst selectivity and stability [21]. This result was observed when the activities of fresh catalysts were compared with the activities of the catalysts after 30 hours of DMDS oxidation. The aim of this study was to apply the developed accelerated ageing protocol to the same catalytic material to gain more information on the deactivation of this material.

The accelerated ageing was carried out for two bimetallic catalysts prepared in the laboratory, i.e. 0.3Pt10Cu/Al and 0.3Pt10Cu/$AlSi_{20}$. The comparison of the activities of fresh catalysts and those undergone the accelerated ageing are presented in Figures 13 and 14.

Figure 13. Light-off tests of DMDS oxidation over fresh and poisoned 0.3Pt10Cu/Al catalysts.

Figure 14. Light-off tests of DMDS oxidation over fresh and poisoned 0.3Pt10Cu/$AlSi_{20}$ catalysts.

Figure Figure 13 shows that the catalytic activity of 0.3Pt10Cu/Al in the oxidation of DMDS has decreased since T_{90} has moved from 310 °C to temperature higher than 400 °C (Table 10). However, the deactivation is not as severe as after 30 h time on stream in DMDS oxidation [21]. In the light-off profile of poisoned 0.3Pt10Cu/Al, we can observe a small discontinuity between 240 and 340°C, which was also observed after 30 h time on stream experiment. This discontinuity could be due to the rearrangement of the catalyst surface due the accelerated ageing, which should be studied more deeply.

Regarding the 0.3Pt10Cu/$AlSi_{20}$ catalyst (Figure 14), the catalytic activity after accelerated ageing seems to be slightly improved at the low temperature range of 240-300 °C. However, when taking into account the repeatability of the light-off tests, clear conclusion cannot be made on this result. At higher temperatures, it was observed that the conversion of DMDS was slightly decreased and T_{90} had moved from 320 °C in the case of the fresh catalyst to 360 °C in the case of the poisoned catalyst (Table 10).

Based on the catalytic activity results, it was clear that the 0.3Pt10Cu/$AlSi_{20}$ catalyst was more stable against the accelerated poisoning treatment. To get more detailed view on the phenomena a series of physico-chemical analysis were made. Elemental analysis by XRF showed that the alumina-silica supported catalyst retained less sulfur (2.7 wt-%) than the alumina supported catalyst (4%), which could explain the different catalytic behavior of the two materials. These results are in accordance with our previous work [21], which showed that the amorphous phase of Al_2O_3-SiO_2 increases the resistance of a supported catalyst against poisoning by sulfur [56,57].

The specific surface area measurements after conducting the accelerated poisoning over the fresh 0.3Pt10Cu/Al and 0.3Pt10Cu/$AlSi_{20}$ catalysts (Table 11) showed that the surface area of 0.3Pt10Cu/$AlSi_{20}$ decreased only by 38% while it was decreased by 41% in the case of the 0.3Pt10Cu/Al catalyst. This finding is in accordance with the XRF analysis result where the sulfur content was higher for the Al_2O_3 supported catalyst. The XRD measurements did not show any obvious changes regarding the new formed phases due to the deposited sulfur.

Based on TEM results, it was revealed that the particles on the surface of the poisoned 0.3Pt10Cu/Al catalyst were exposed to sintering where the size is about 100 nm (Figure 15.a) compared to the fresh one in our previous work [21], moreover, and according to the Table 12, the poisoned 0.3Pt10Cu/Al catalyst exhibited relatively high sulfur content and that sulfur was found to be presented on both, the active phase and the support material.

Figure 15. TEM images of a) poisoned 0.3Pt10Cu/Al and b) poisoned 0.3Pt10Cu/$AlSi_{20}$ catalyst.

For the poisoned 0.3Pt10Cu/$AlSi_{20}$ catalyst, there was an appearance of bimetallic particles on the surface, as the Figure 15.b and EDS 1-b from Table 12 showed. The mixed Pt-Cu particle exhibited a bigger size of 10 nm meaning that some particles were exposed to the sintering. Another important finding is that sulfur content in this catalyst was very low compared to the one in poisoned 0.3Pt10Cu/Al catalyst, this result will be inspected in the incoming chapters by other techniques as well.

In addition to TEM, FESEM was used to analyze the topographic microstructure of the surface of the poisoned 0.3Pt10Cu/$AlSi_{20}$ and 0.3Pt10Cu/Al catalysts. For the poisoned 0.3Pt10Cu/Al catalyst, the elemental mapping by FESEM showed (Figure not shown) the presence of Pt in two very small

areas. Concerning sulfur, it was found to be dispersed over the entire surface of the poisoned 0.3Pt10Cu/Al catalyst and located on the same area where O and Al were.

For the poisoned 0.3Pt10Cu/$AlSi_{20}$ catalyst (Figure not shown), it was clearly seen that sulfur took the same localization as Si, Al, O and Cu on the surface of the catalyst, which can allow saying that S is dispersed on the catalyst surface, but at a lower concentration than in the case of the poisoned 0.3Pt10Cu/Al catalyst as the TEM-EDX and XRF (for bulk S content) analyses showed.

To get more compound-specific information on the poisoning of 0.3Pt10Cu/Al and 0.3Pt10Cu/$AlSi_{20}$ catalysts, XPS measurements were carried out for fresh and poisoned samples. The decomposition spectra of the individual components of Pt $4d_{5/2}$ show the presence of three different species of platinum in the case of the fresh 0.3Pt10Cu/Al catalyst (Figure 16.a). The spectral peak ($Pt4d_{5/2}$) with BE at around 315.2 eV is associated with the chemical state of Pt (0) and the last peak at 319 eV is derived from the existence of oxidized platinum species (PtO_2). The third peak centered at 312.6 eV corresponds to Pt (0) belonging to the Pt-Cu alloy or intermetallic compounds of Pt-Cu [58]. The binding energy of $Pt4d_{5/2}$ of about 317.2 eV for the fresh 0.3Pt10Cu/$AlSi_{20}$ catalyst (Figure 17.a) indicates that Pt is present likely in an oxidized form of PtO [59].

Concerning both the poisoned 0.3Pt10Cu/Al and 0.3Pt10Cu/$AlSi_{20}$ catalysts, the same results were found. The decomposition of the spectra of individual components of Pt $4d_{5/2}$ showed the presence of two platinum species in both cases (Figures 16.b and 17.b). The spectral peak ($Pt4d_{5/2}$) of poisoned 0.3Pt10Cu/Al catalyst (Figure 16.b) with BE at around 315.2 eV is associated with the chemical state of Pt (0) and the last peak at 319 eV is derived from the existence of oxidized platinum species (PtO_2). The third peak centered at 312.6 eV corresponds to Pt (0) belonging to the Pt-Cu alloy or intermetallic compounds of Pt-Cu [58]. The spectral peak ($Pt4d_{5/2}$) of poisoned 0.3Pt10Cu/$AlSi_{20}$ catalyst (Figure 17.b) was found to exist with the BE at around 315 eV, which is associated to the chemical state of Pt(0) and the last peak at 318.5 eV can correspond to either Pt(IV) or to the platinum species interacting with SO_2^{-4} on the support surface [56].

Figure 16. Decomposition of Pt $4d_{5/2}$ of a) fresh 0.3Pt10Cu/Al b) Pt 4d of poisoned 0.3Pt10Cu/Al.

Figure 17. Decomposition of a) Pt $4d_{5/2}$ of fresh 0.3Pt10Cu/$AlSi_{20}$ and b) Pt $4d_{5/2}$ of poisoned 0.3Pt10Cu/$AlSi_{20}$ catalysts.

Concerning copper in all fresh and poisoned catalysts, the most intense peak (Cu $2p_{3/2}$) of the Cu 2p line, has a binding energy at around 933.68 to 933.8 eV and the appearance of satellite lines on each Cu2p component prove that copper is present in the form of CuO in both fresh and poisoned catalysts [60].

According to the decomposition of the individual components of S 2p (Figures 18.a and b), the binding energy of the S $2p_{1/2}$ at 168.9 eV, showed that sulfur is present only in the form of S^{6+}[52-55], as proved by the presence of a single transition of S $2p_{1/2}$ and S $2p_{3/2}$ in both the cases.

Figure 18. Decomposition of a) S2p of poisoned 0.3Pt10Cu/Al and b) S2p of poisoned 0.3Pt10Cu/$AlSi_{20}$.

After carrying out the accelerated laboratory ageing on 0.3Pt10Cu/Al and 0.3Pt10Cu/$AlSi_{20}$ catalysts, it was noted that the concentration of the active phase on the surface was changed in the case of 0.3Pt10Cu/Al. According to Table 13, the atomic ratio of Pt/Al (0.0022) and Cu/Al (0.09) has decreased, indicating that the surface of the same catalyst has been exposed to some chemical poisoning, most likely sulfur species coming from SO_2.

In the case of 0.3Pt10Cu/$AlSi_{20}$, the atomic ratio decrease of Pt/Al (0.0035) and Cu/Al (0.12) was detected as well, but it was not as significant as in the case of the 0.3Pt10Cu/Al catalyst. Furthermore, the concentration of elemental sulfur on the 0.3Pt10Cu/Al surface was slightly higher (0.1) than that found in the case of the 0.3Pt10Cu/$AlSi_{20}$ (0.08) catalyst.

The presence of Pt (0) and Pt (IV) species on the surface of the support can provide an environment in which SO_2 interactions are faster. It is known that the oxidation of SO_2 to SO_3 is catalyzed by Pt at temperatures higher than 200 °C [61-63]. The formed SO_3 can then react with the Al_2O_3 support to form $Al_2(SO_4)_3$. This reaction is further catalyzed by the presence of Pt [62]. The oxidation of SO_2 occurs via dissociative adsorption on Pt [55, 52, 53] and it may be increased over Pt(0) compared to Pt(IV) due to the higher electronic density in Pt(0), and thus, leading to higher interactions of Pt binding electrons with the anti-bonding orbital of the SO_2 molecule.

It has been also observed that sulfate promotes the Pt mobility, which can lead to Pt agglomeration and a loss in active surface area. Besides, Pt crystals cannot be properly re-dispersed whilst sulfate is present on the catalyst surface. According to the study of Koro *et al.*, the most sensitive and vulnerable catalyst against sulfur is the one that contains high oxidation states of Pt on the surface [21, 64]. This is in agreement with what has been observed related to the 0.3Pt10Cu/Al catalyst, which showed the presence of species of Pt(IV), and also a higher concentration of sulfur on its surface in comparison to the 0.3Pt10Cu/$AlSi_{20}$ catalyst that contained Pt^{2+}on its surface.

When comparing the catalytic performances of the two bimetallic catalysts (0.3Pt10Cu/$AlSi_{20}$ and 0.3Pt10Cu/Al) after accelerated ageing, it has been found that the $AlSi_{20}$ support has played a very important protective role against the poisoning of the active surface by sulfur compounds. It is most probably due to its highly acidic surface nature.

3. Conclusion

Based on the catalytic activity tests and the structural and textural information obtained by different characterization methods, it can be stated that the accelerated deactivation procedure has led to a similar type of catalyst deactivation as the industrial scale deactivation and this has happened especially in a qualitative way. It was observed that the decrease in the activity of industrially aged Pt/Al catalyst was originating from the decrease in the active surface area due to support sintering, chemical poisoning originating from sulfate formation (on both support and the active phase), increase in Pt particle size and formation of highly oxidized Pt(IV) species that are less tolerant

against sulfur. After accelerated ageing of Pt/Al catalyst, the same phenomena were present in qualitative manner and the method was used in the ageing of new more sulfur tolerant materials.

In the second part, the present study confirmed the beneficial role of the addition of 20 mol-% of SiO_2 into the alumina support. The accelerated deactivation of the 0.3Pt10Cu/Al and 0.3Pt10Cu/$AlSi_{20}$ catalysts showed that the $AlSi_{20}$ supported catalyst was the most stable and resistant against sulfur deactivation as it was expected. For example, $AlSi_{20}$ supported catalyst retained remarkably less sulfur than Al-supported catalyst. In addition, the sintering of Pt was reduced when it was supported on $AlSi_{20}$. Although the accelerated deactivation was able to represent the industrial ageing in qualitative way, as the next step for the development of the accelerated ageing, a thermal treatment of the catalyst before poisoning procedure will be done.

Acknowledgements

The authors would like to thank support of M.Sc. Markus Riihimäki for XRF and M.Sc. Santtu Heinilehto for XPS analyses.

References

[1] K.R. Smith, Proc. Natl. Acad. Sci. USA 97 (2000) 13286.

[2] Y. Nagata, Measurement of odor threshold by triangle odor bag method. Odor Measurement Review, Japan Ministry of the Environment (2003) 118-127.

[3] J.J. Spivey, Solid catalyst for the oxidation of volatile organic compounds, in: B. Gerhard (Ed.), Handbook of Heterogeneous Catalysis, second ed., vol. 5, 2008, pp. 2394-2411.

[4] G.A. Smook, Handbook for pulp & paper technologists, 3rd ed., Angus Wilde Publications, Vancouver (2002).

[5] S. Vigneron, P. Deprelle, J. Hermia, Catal. Today 27 (1996) 229-236.

[6] J.J. Spivey, J.B. Butt, Catal. Today 11 (1992) 465-500.

[7] T. Barakat, J.C. Rooke, H.L. Tidahy, M. Hosseini, R. Cousin, J.-F. Lamonier, J.-M. Giraudon, G. De Weireld, B.-L. Su, S. Siffert, ChemSusChem 4 (2011) 1420-1430.

[8] F. Wyrwalski, J.-M. Giraudon, J.-F. Lamonier, , Catal. Lett. 137 (2010) 141-149.

[9] T. Watanabe, K. Kawashima, Y. Tagawa, K. Tashiro (2007) SAE Paper 2007-01-1920.

[10] T. Mishra, P. Mahapatra, K.M. Parida, Appl. Catal. B: Environ. 79 (2008) 279-285.

[11] S. Azalim, M. Franco, R. Brahmi, J.-M. Giraudon, J.-F. Lamonier, J. Hazard. Mater. 188 (2011) 422-427.

[12] S.C. Kim, W.G. Shim, Appl. Catal. B: Environ. 98 (2010) 180–185.

[13] M. Ferrandon, J. Carno, S. Jaras, E. Bjornbom, Appl. Catal. A: Gen. 180 (1999) 141-151.

[14] J. Lojewska, A. Kolodziej, J. Zak, J. Stoch, Catal. Today 105 (2005) 655-661.

[15] B. Aellach, A. Ezzamarty, J. Leglise, C. Lamonier, J.-F. Lamonier, Catal. Lett. 135 (2010) 197-206.

[16] F. Wyrwalski, J.-M. Giraudon, J.-F. Lamonier, Catal. Lett. 137 (2010) 141-149.

[17] L. Tidahy, S. Siffert, F. Wyrwalski, J.-F. Lamonier, A. Aboukaïs, Catal. Today 119 (2007) 317-320.

[18] W. Li, S.T. Oyama, ACS Symposium, Washington, DC 41 (1996) 14.

[19] A.K. Neyestanaki, F. Klingstedt, T. Salmi, D.Y. Murzin, Fuel (2004) 83:395.

[20] F.C. Galisteo, R. Mariscal, M.L. Granados, Z. Poves, J.L.G. Fierro, V. Kröger, Keiski R.L. Appl Catal B (2007) 72:272.

[21] B. Darif, S. Ojala, L. Pirault-Roy, M. Bensitel, R. Brahmi, R. L. Keiski., Appl. Catal. B: Environ. 181 (2016) 24–33.

[22] C.H. Bartholomew, G.A. Fuentes, Eds., Studies in Surf. Sci. and Catal. 111 (1997) 585–592.

[23] S. Ojala, U. Lassi, R. Ylönen, R.L. Keiski, Tappi J 4 (2005) 9-14.

[24] S. Ojala, U. Lassi, M. Härkönen, T. Maunula, R. Silvonen, R. L. Keiski, Chem. Eng. J 120 (2006) 11–16.

[25] S.J. Gregg, K.S.W. Sing, Adsorption, Surface and Porosity, 2nd ed; Academic Press: London, UK, 1982.

[26] K.S.W. Sing, D.H. Everett, R.A.W. Haul, L. Moscou, R.A. Pierotti, J. Rouquerol, T. Siemieniewska, Pure Appl. Chem 57 (1985) 603–619.

[27] A. Popat, J. Liu, G.Q. Lu, S.Z. Qiao, J. Mater. Chem 22 (2012) 11173-11178.

[28] C.X. Lin, P. Yuan, C.Z. Yu, S.Z. Qiao, G.Q. Lu, Micropor. Mesopor. Mat. 126 (2009) 253–261.

[29] Z. Yuan, T. Ren, A. Azioune, and J. Pireaux, Chem. Mater 18 (2006) 1753-1767.

[30] C. Sangwichien, G. L. Aranovich, and M. D. Donohue, Colloids Surfaces A: Physicochem. Eng. Asp. 206 (2002) 313-320.

[31] A. Russell, W.S. Epling, Catal Rev Sci Eng 53 (2011) 337.

[32] C.H. Bartholomew, Appl Catal A: Gen 212 (2001) 17.

[33] G. Cavataio, H-W. Jen, J.W. Girard, D. Dobson, J.R. Warner, C.K. Lambert, SAE Paper (2009) 2009-01-0627.

[34] A.K. Neyestanaki, F. Klingstedt, T. Salmi, D.Y. Murzin, Fuel (2004) 83:395.

[35] R.T. Baker, C.H. Bartholomew, D.B. Dadyburjor, J.A. Horsley, Ed.; Catalytica: Mountain View, CA, USA, 1991; pp. 169-225.

[36] C.H. Bartholomew, In: Eds. J.J Spivey, S.K. Agarwal, Specialist Periodical Report; Royal Society of Chemistry, Cambridge, UK 10 (1993) 41–82

[37] C.H. Bartholomew, Appl. Catal. A 107 (1993) 1–57.

[38] C.H. Bartholomew, Studies in Surf. Sci. and Catal. 88 (1994) 1–18.

[39] C.H. Bartholomew, Studies in Surf. Sci. and Catal. 111 (1997) 585–592.

[40] D.S. Tucker, A. Bleier, J. Am. Ceram. Sc 68 (1985) 163-164.

[41] C. Pecharromán ,I. Sobrados , J. E. Iglesias , T. González-Carreño , J. Sanz, J. Phys. Chem. B, 103 (1999) 6160–6170.

[42] P. Mishra, Mater. Lett. 55 (2002) 425–429.

[43] W.H. Gitzen, Alumina as a Ceramic Material. American Ceramic Society; Columbus, OH, USA: 1970.

[44] D.J. Young, High Temperature Oxidation and Corrosion of Metals. Elsevier; Oxford, 2008.

[45] S.R.J. Saunders, M. Monteiro, F. Rizzo, Progress in Materials Science 53 (2008) 775-837.

[46] A. Winkler, D. Ferri, M. Aguirre, Appl. Catal. B 93 (2009) 177.

[47] J.D. Peter-Hoblyn, J.M. Valentine, B.N. Sprague, W.R. Epperly, Methods for reducing harmful emissions from a diesel engine. U.S. Patent 6,003,303, 21 December 1999.

[48] I. Manson, Self-regenerating diesel exhaust particulate filter and material. U.S. Patent 6,013,599, 11 January 2000.

[49] M. Deeba, Y.K. Lui, J.C. Dettling, Four-way diesel exhaust catalyst and method of use. U.S. Patent 6,093,378, 25 July 2000.

[50] J.A. Moulijn, A.E. van Diepen, F. Kapteijn, Appl. Catal. A: Gen 212 (2001) 3–16.

[51] M. G. Kim, H. S. Kim, Y. G. Ha, J. He, M. G. Kanatzidis, A. Facchetti, T. J. Marks, J. Am. Chem. Soc. 132 (2010) 10352-10364.

[52] U. Kohler, H.W. Wassmuth, Surf. Sci. 122 (1982) 491.

[53] R.C. Ku, P. Wynblatt, Appl. Surf. Sci. 8 (1981) 250.

[54] D. Briggs, M.P. Seah (Eds.), Practical Surface Analysis by Auger and X-ray Photoelectron Spectroscopy, 2nd ed., Wiley, Chichester, UK, 1990.

[55] C.D. Wagner, W.M. Riggs, L.E. Davis, J.F. Moulder (Eds.), Handbook of X-ray Photoelectron Spectroscopy, Perkin-Elmer Corporation, USA, 1990.

[56] L.V. Duong , B.J. Wood , J.T. Kloprogge, Materials Letters 59 (2005) 1932–1936.

[57] W.R.A.M. Robinson, J.A.R. van Veen, V.H.J. de Beer, R.A. van Santen, Fuel Process. Technol. 61 (1999) 61.

[58] L. E. Gómez, B. M. Sollier, M. D. Mizrahi, J. M. Ramallo López, E. E. Miró, A. V. Boix, INT J. Hydrogen. Energ. 39 (2014) 3719-3729.

[59] G. Corro, J.L.G. Fierro, V. C. Odilon, Catal. Comm. 4 (2003) 371-376.

[60] H-H. Tseng, H-Y. Lin, Y-F. Kuo, Y-T. Su, Chem Eng J 160 (2010) 13-19.

[61] G.C. Bond, Catalysis by Metals, Academic Press, London, 1962.

[62] G.I. Godolets, Stud. Surf. Sci. Catal. 15 (1983) 365.

[63] D.D. Beck, M.H. Kruger, D.R. Monroe, SAE Paper no. 910844 (1991).

[64] G. Corro, J.L.G. Fierro, V. C. Odilon, Catalysis Communications 4 (2003) 371-376.

List of Table captions

Table 1. Light-off test temperatures; comparison of T_{50} and T_{90} in the oxidation of DMDS over fresh and used Pt/Al catalysts.

Table 2. BET-BJH *r*esults of the fresh and used Pt/Al catalysts.

Table 3. $T_{melting}$, T_{Tamman} and $T_{Hüttig}$ values (K) of metals and their compounds, relevant for heterogeneous catalysis [48].

Table 4. EDS analysis from different Pt particles on the surface of the used Pt/Al catalyst.

Table 5. Atomic ratios of the fresh and used Pt/Al catalysts by XPS.

Table 6. Light-off test temperatures comparison (T_{50} and T_{90}) in the oxidation of DMDS over fresh, used and poisoned Pt/Al catalysts.

Table 7. Results of BET-BJH of the fresh, used and poisoned Pt/Al catalysts.

Table 8. EDS measurements for different Pt particles on the surface of the poisoned Pt/Al catalyst.

Table 9. Atomic ratios of fresh, used and poisoned Pt/Al catalysts by XPS

Table 10. T_{90} and T_{50} of DMDS oxidation over fresh and poisoned 0.3Pt10Cu/Al and 0.3Pt10Cu/$AlSi_{20}$ catalysts.

Table 11. Results of BET-BJH of fresh and poisoned 0.3Pt10Cu/Al and 0.3Pt10Cu/$AlSi_{20}$catalysts.

Table 12. EDS measurements for different Pt particles on the surface of the poisoned 0.3Pt10Cu/Al and 0.3Pt10Cu/$AlSi_{20}$ catalyst.

List of Figure captions

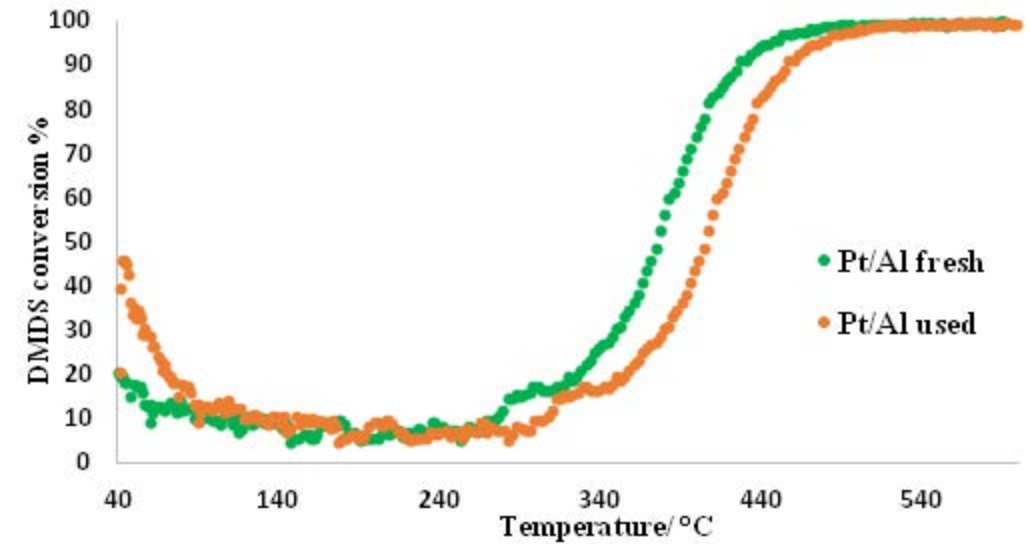
DMDS conversion %
100
90
80
70
60
50
40
30
20
10
0
40
140
240
340
440
540
Temperature/ °C
Pt/Al fresh
Pt/Al used

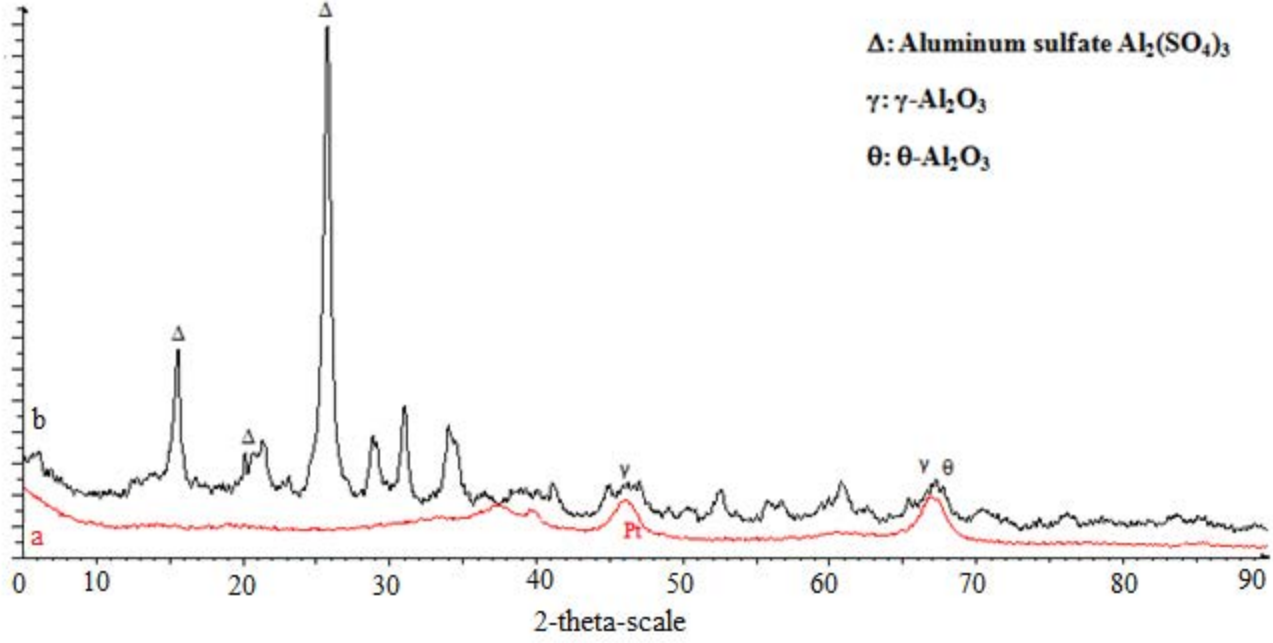
Δ: Aluminum sulfate $Al_2(SO_4)_3$
γ: γ-Al_2O_3
θ: θ-Al_2O_3
Δ
Δ
Δ
b
a
γ
γ θ
Pt
0
10
20
30
40
50
60
70
80
90
2-theta-scale

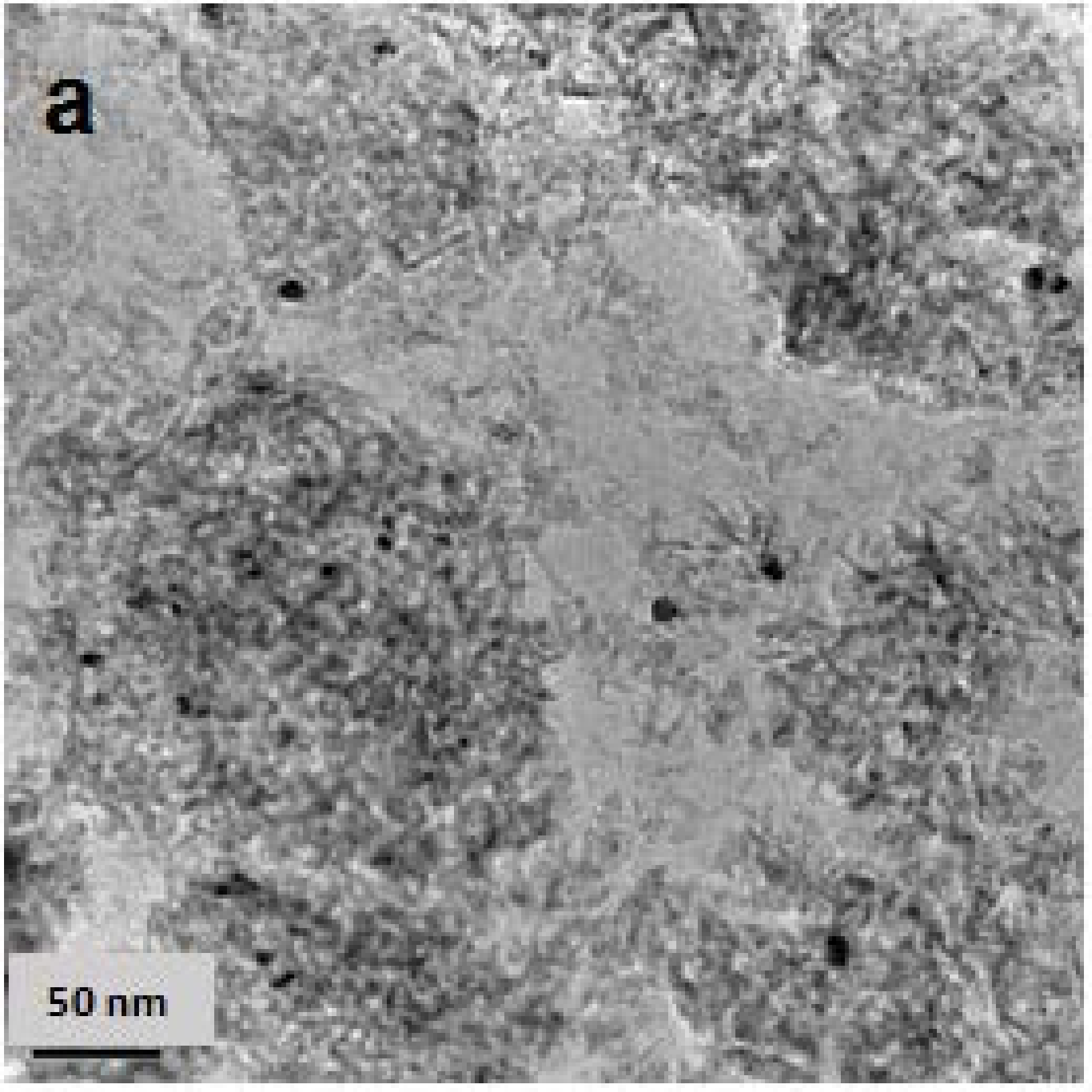
a
50 nm

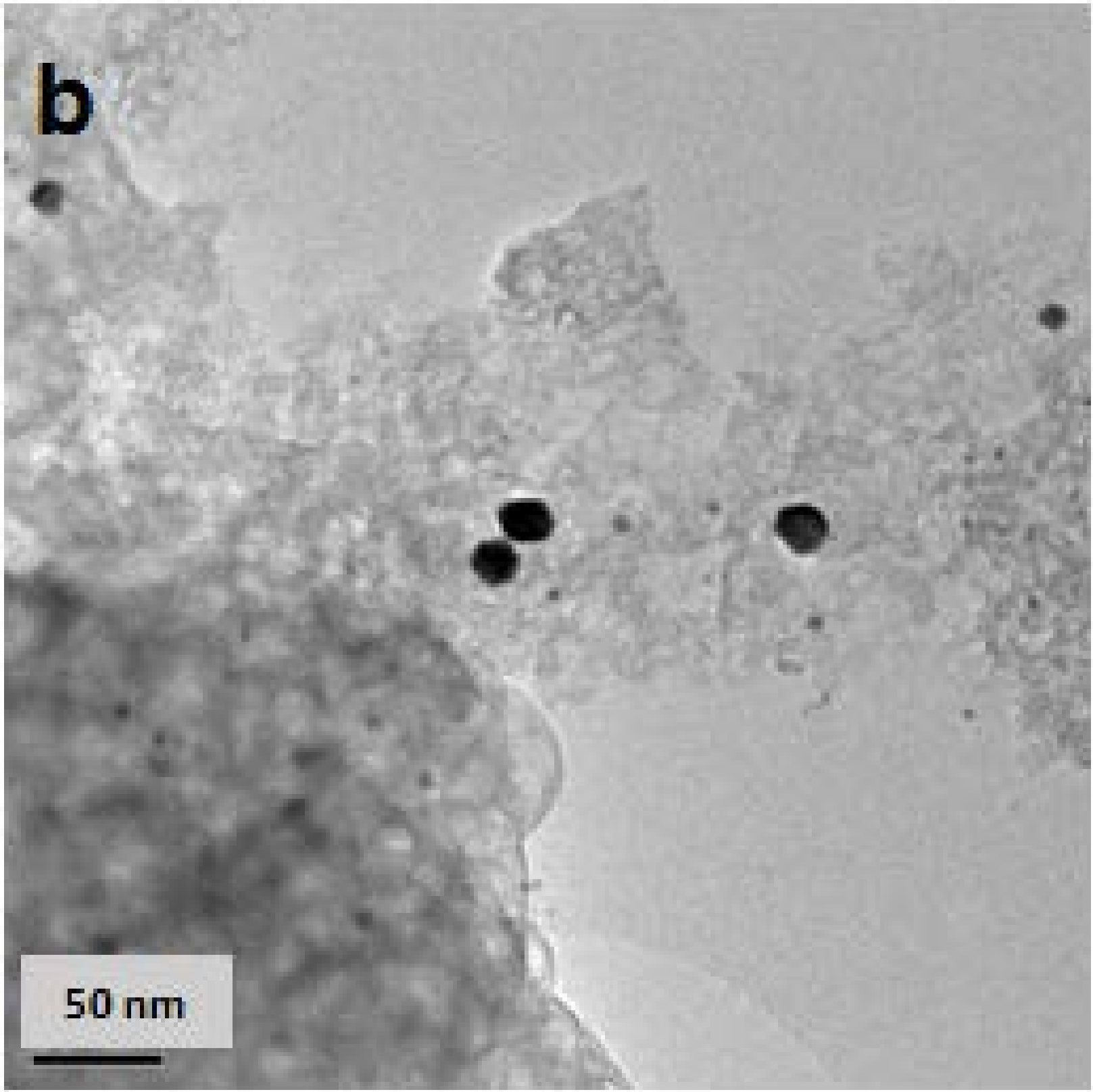
b
50 nm

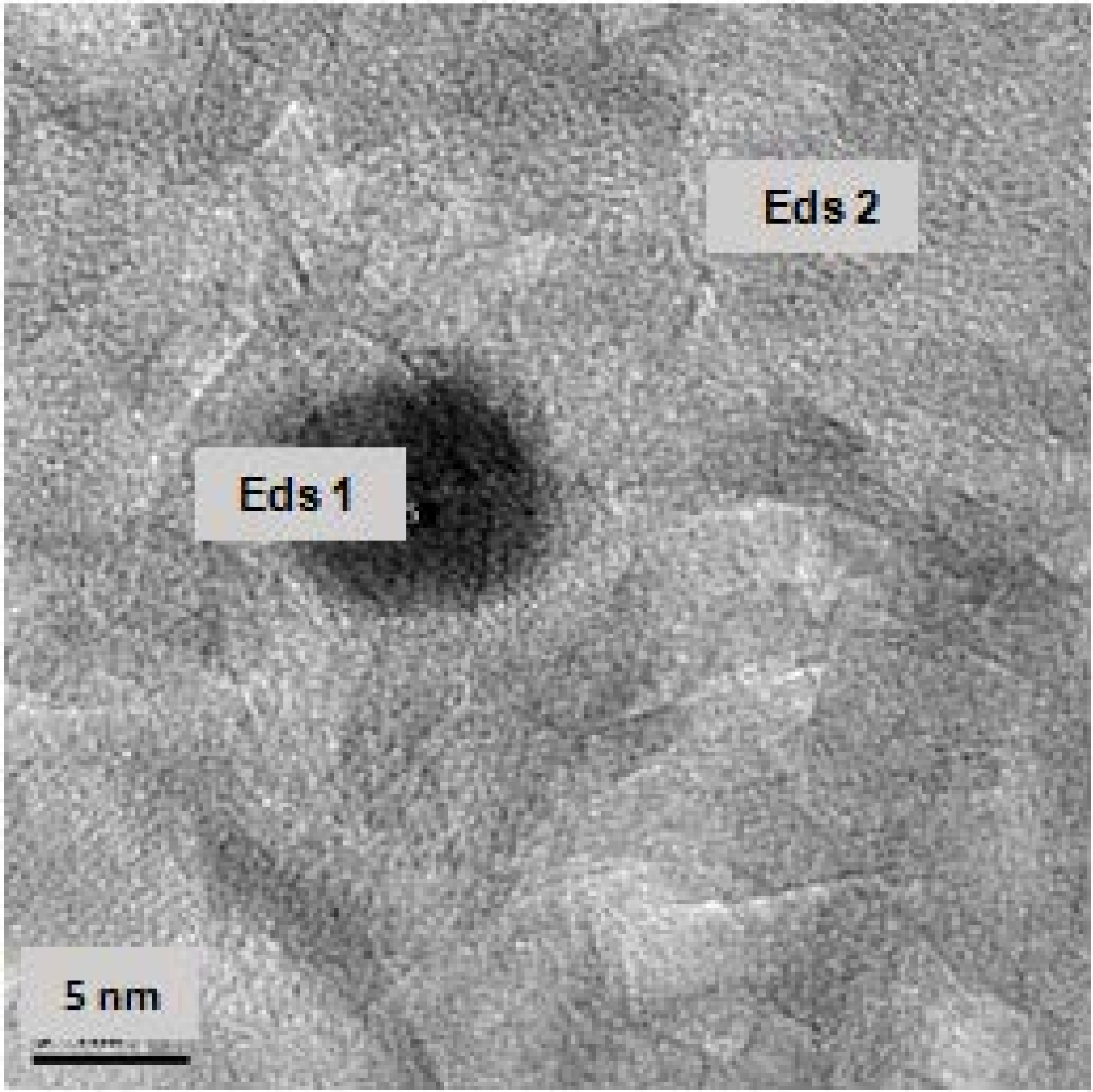
Eds 2
Eds 1
5 nm

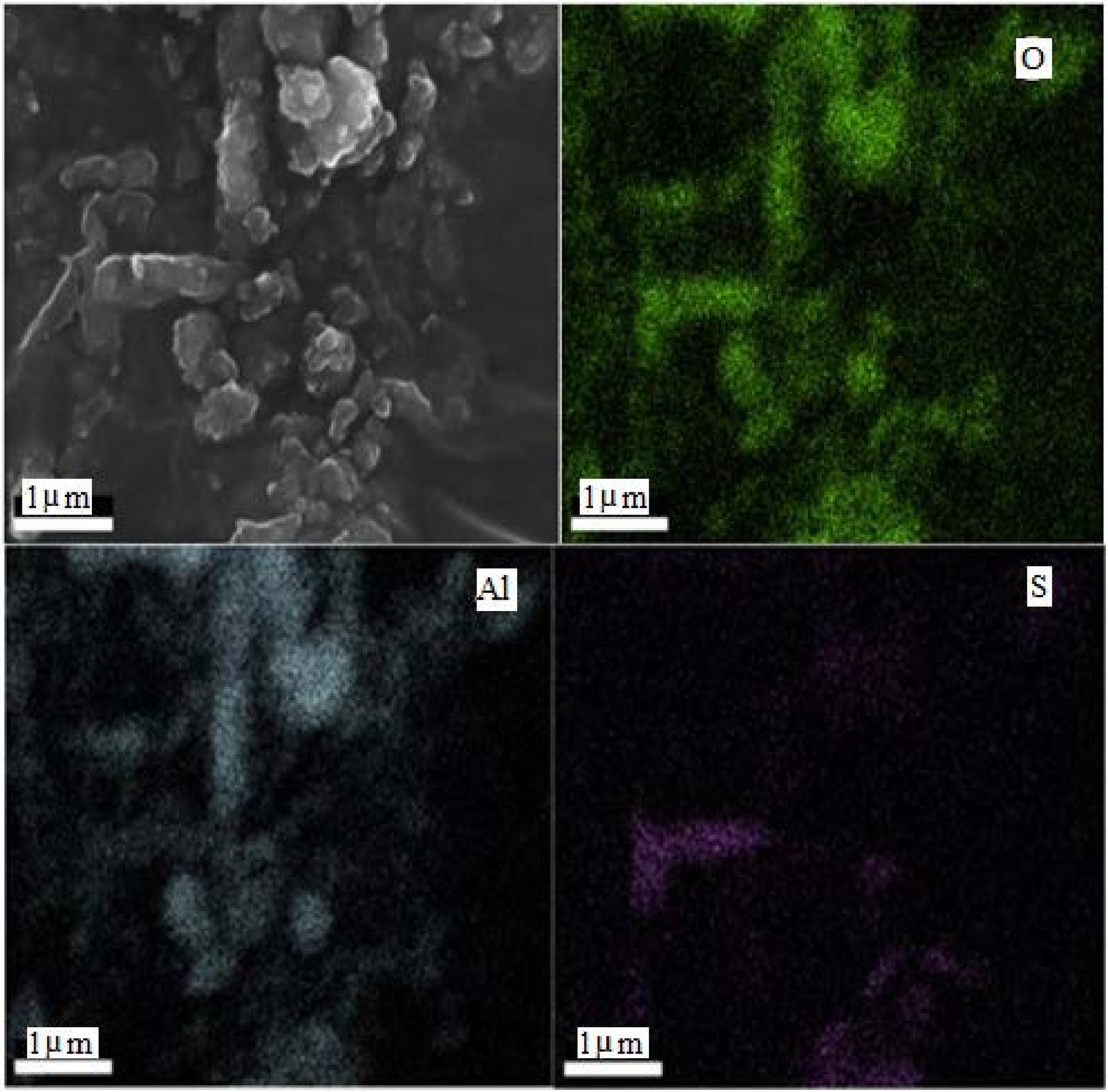
1 μm
O
1 μm
Al
1 μm
S
1 μm

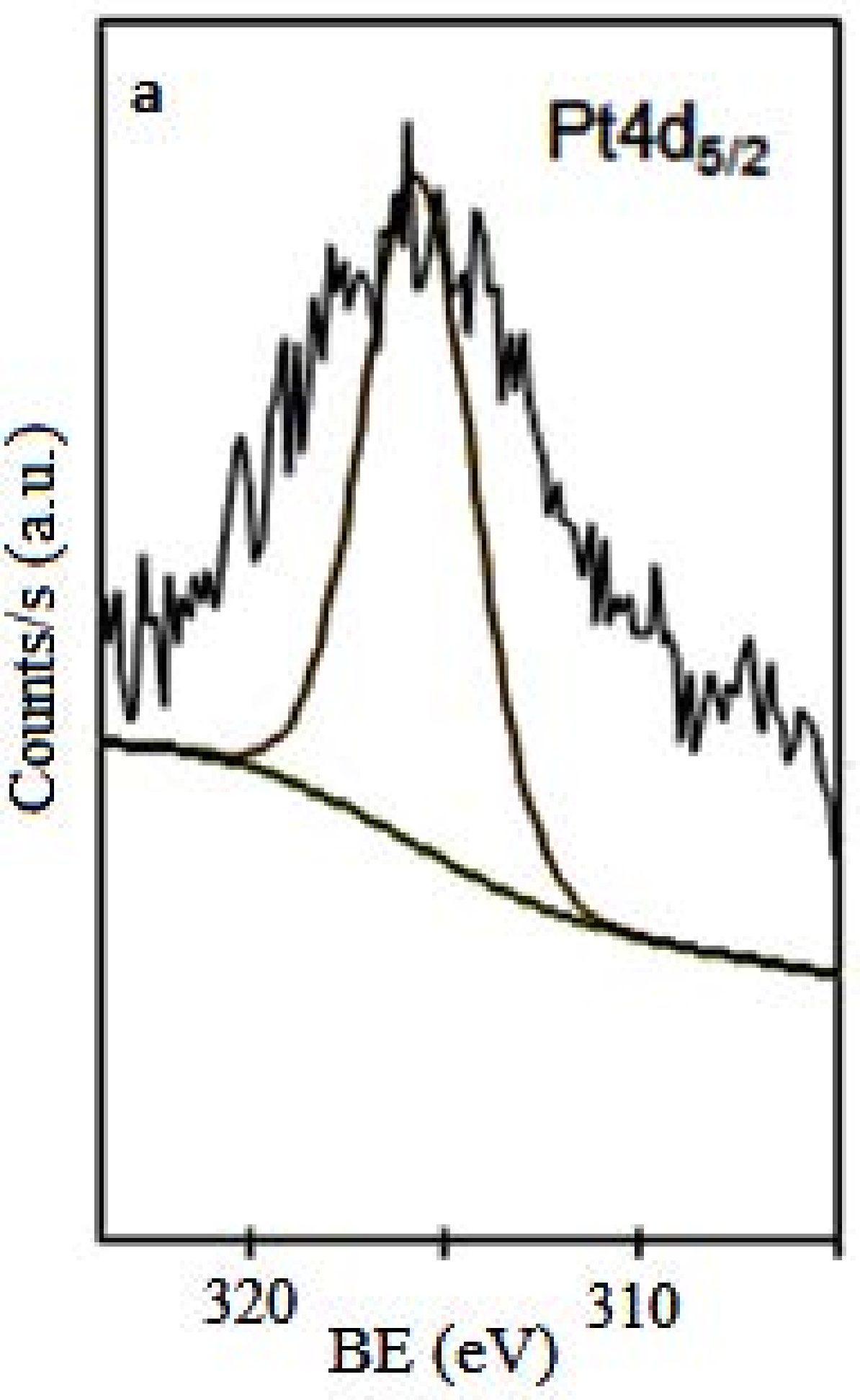
a
Pt4d5/2
Counts/s (a.u.)
320
310
BE (eV)

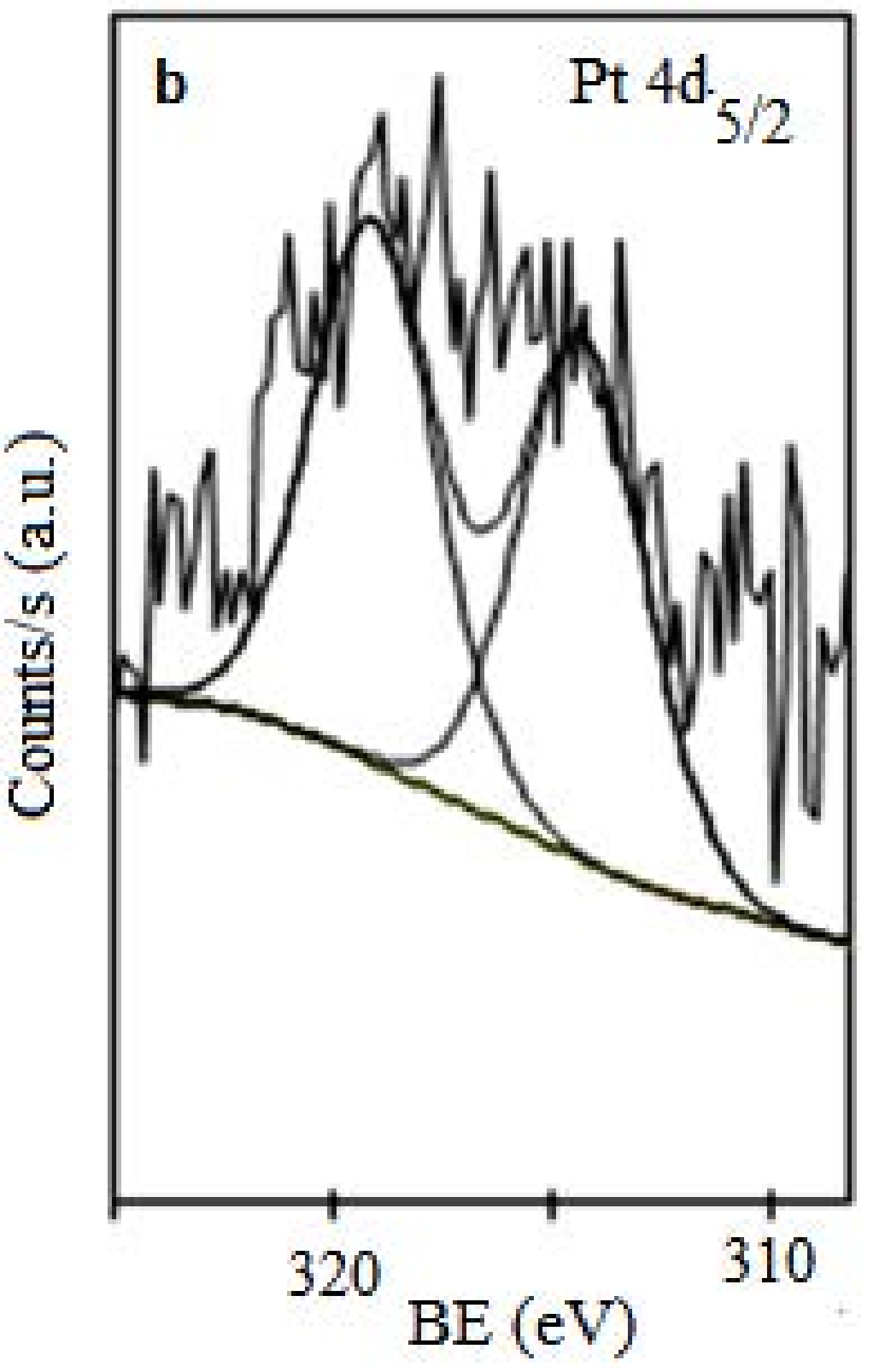
b
Pt 4d5/2
Counts/s (a.u.)
320
310
BE (eV)

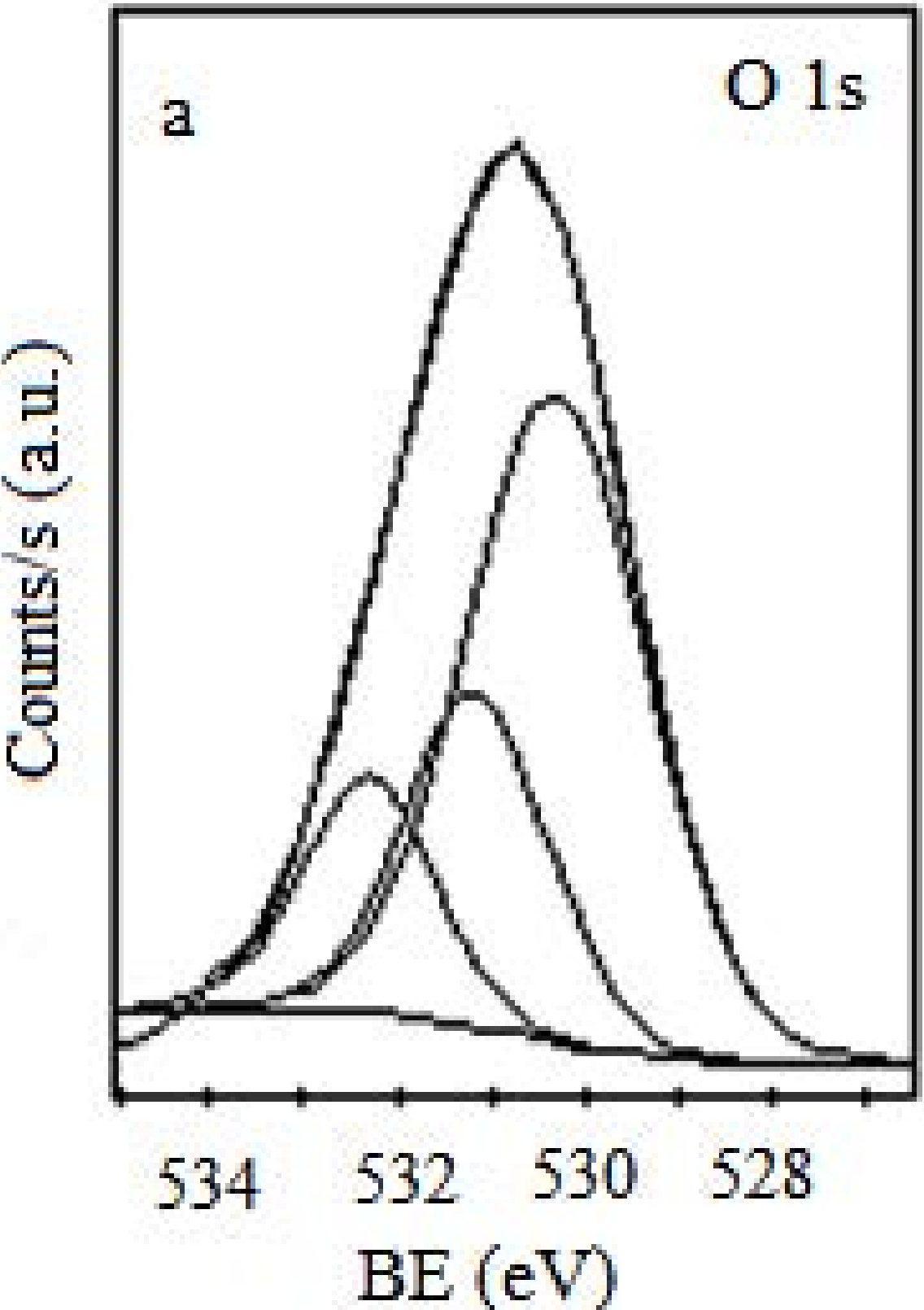
a
O 1s
Counts/s (a.u.)
534
532
530
528
BE (eV)

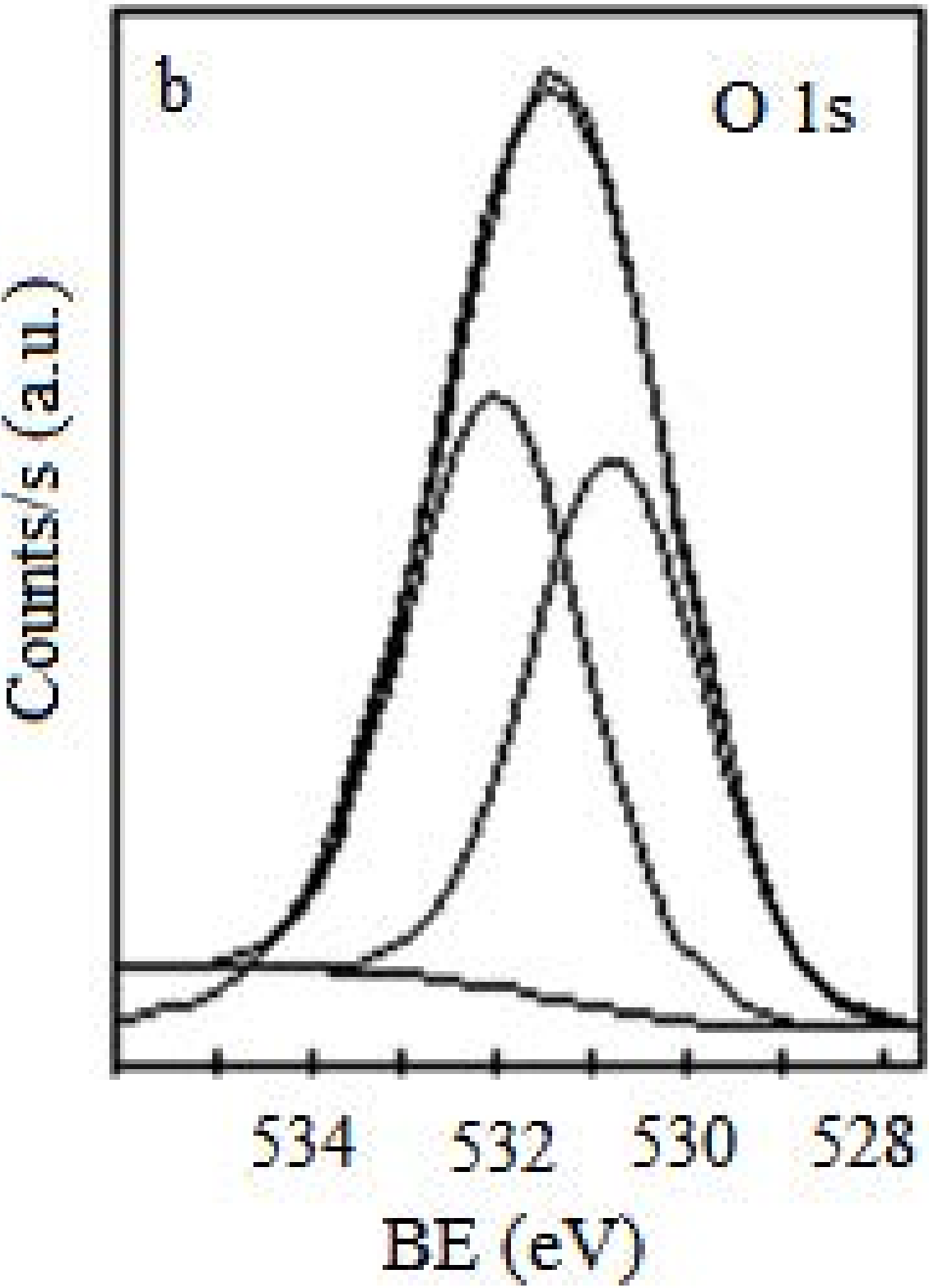
b
O 1s
Counts/s (a.u.)
534
532
530
528
BE (eV)

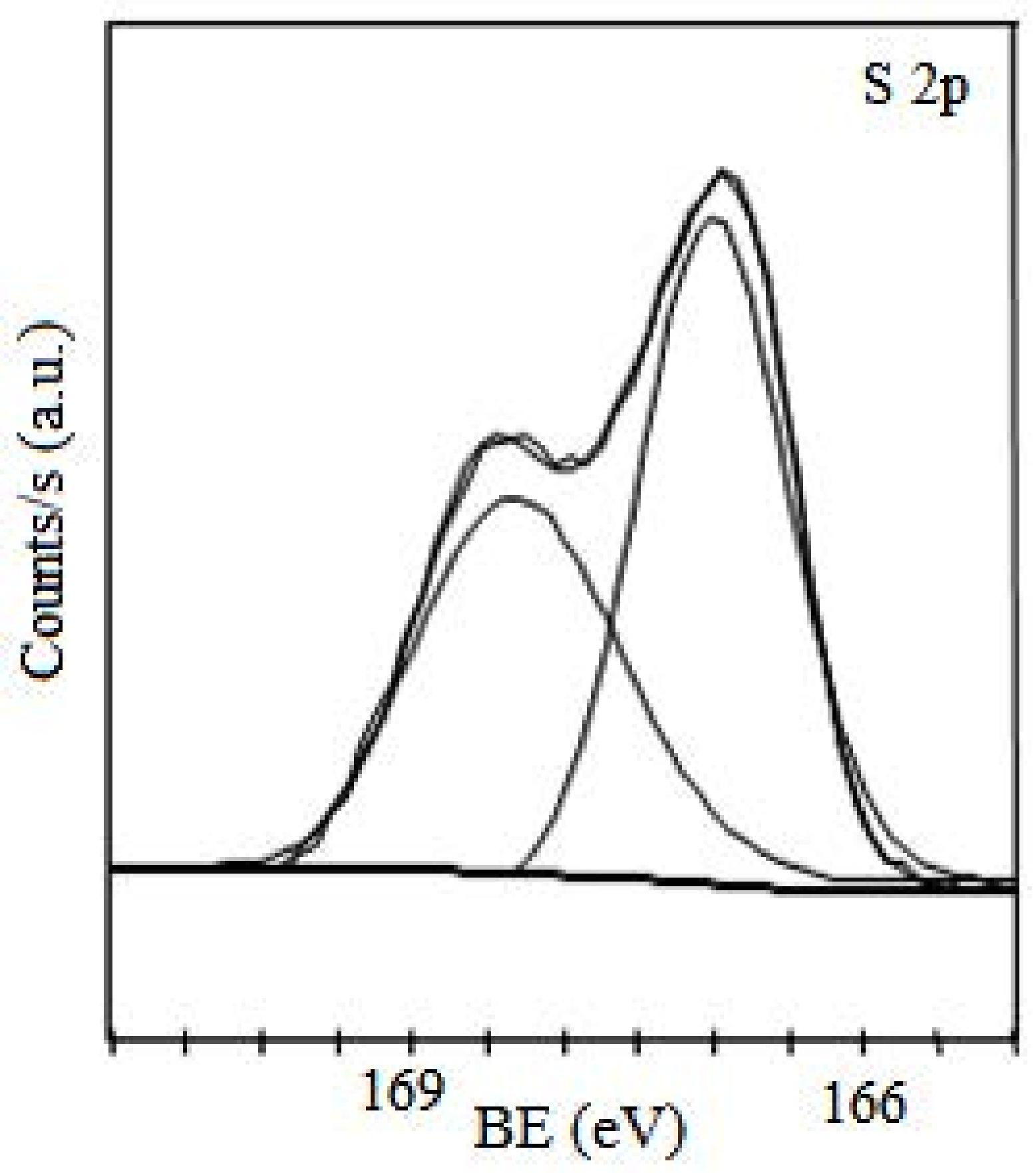
S 2p
Counts/s (a.u.)
169
BE (eV)
166

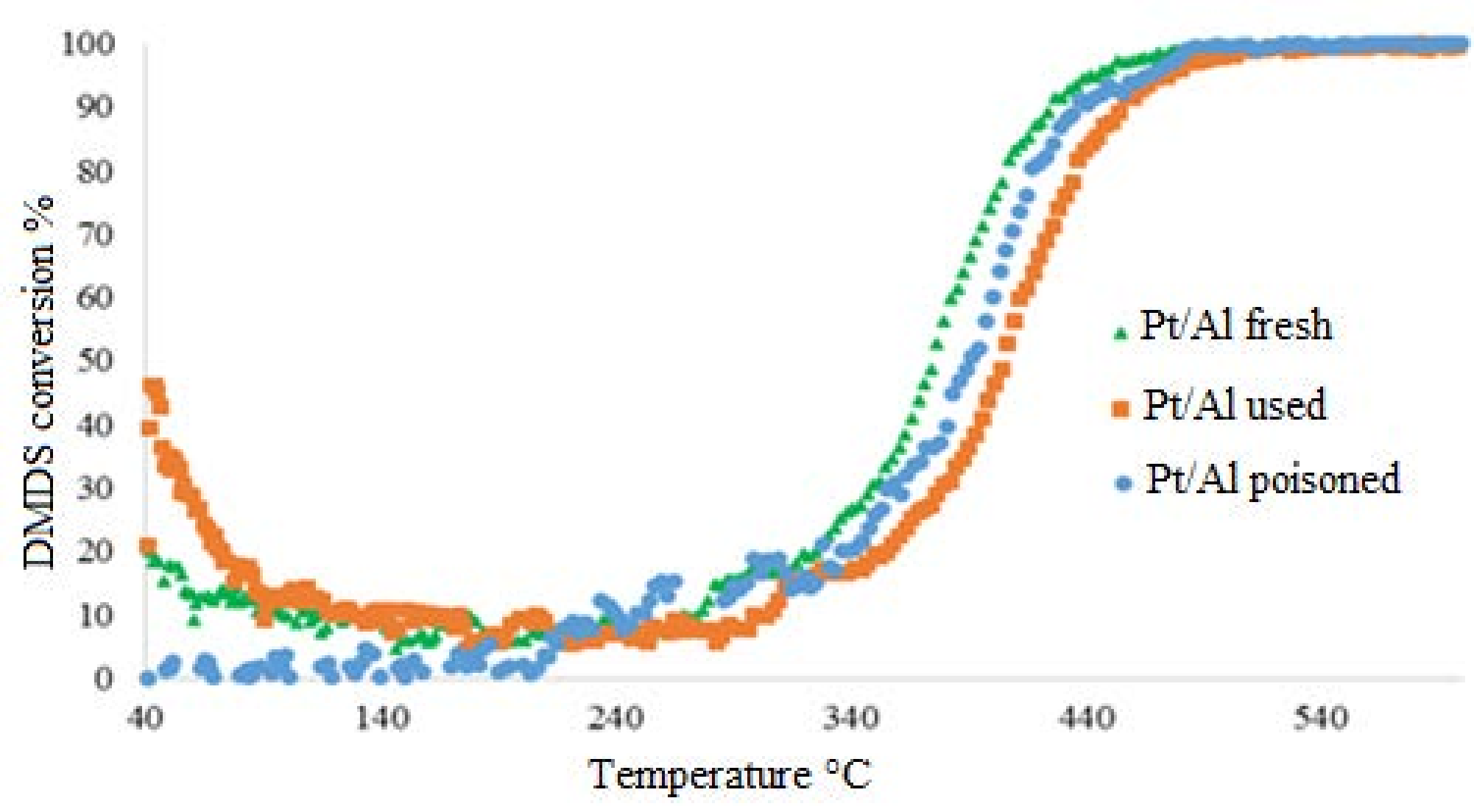
DMDS conversion %
100
90
80
70
60
50
40
30
20
10
0
40
140
240
340
440
540
Temperature °C
Pt/Al fresh
Pt/Al used
Pt/Al poisoned

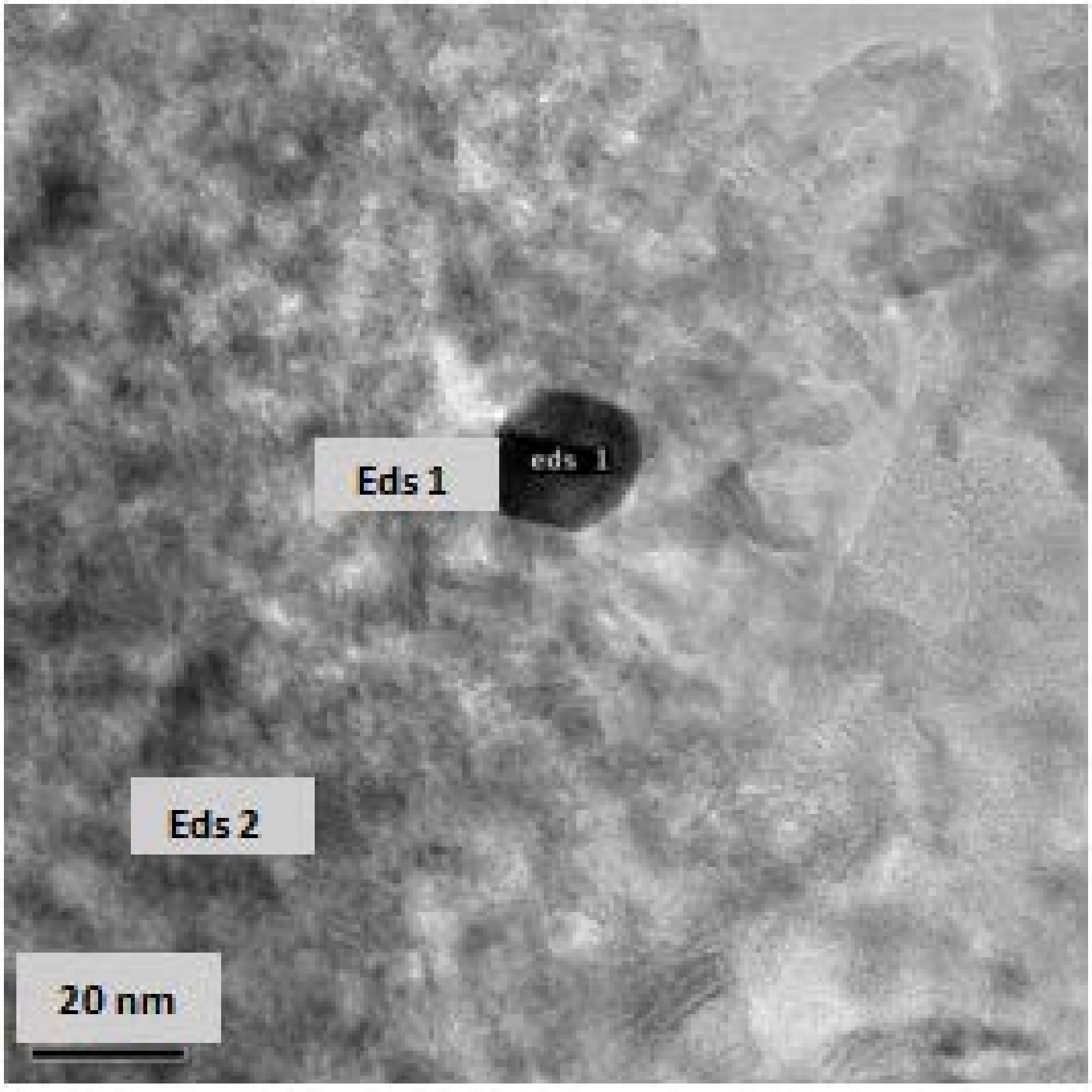
Eds 1
eds 1
Eds 2
20 nm

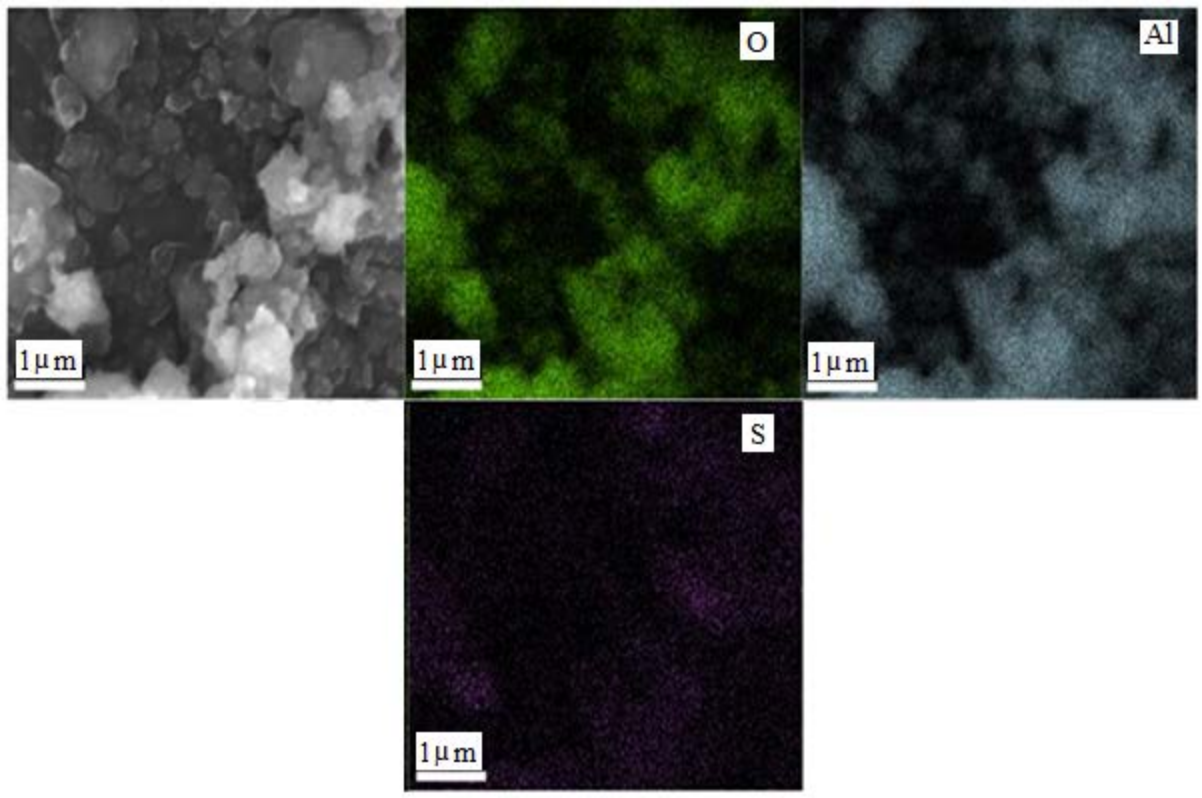
1μm
O
1μm
Al
1μm
S
1μm

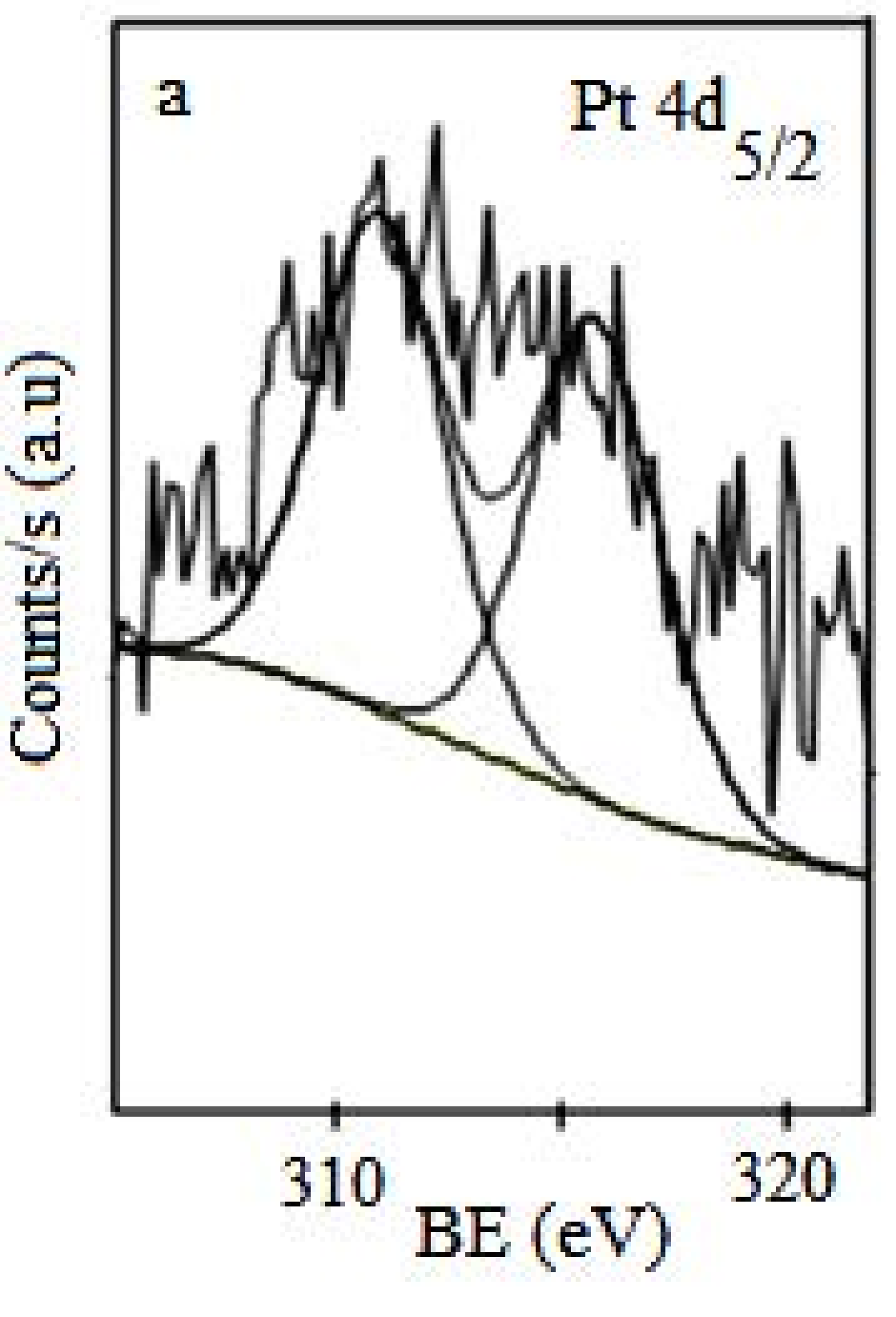
a
Pt 4d 5/2
Counts/s (a.u)
310
320
BE (eV)

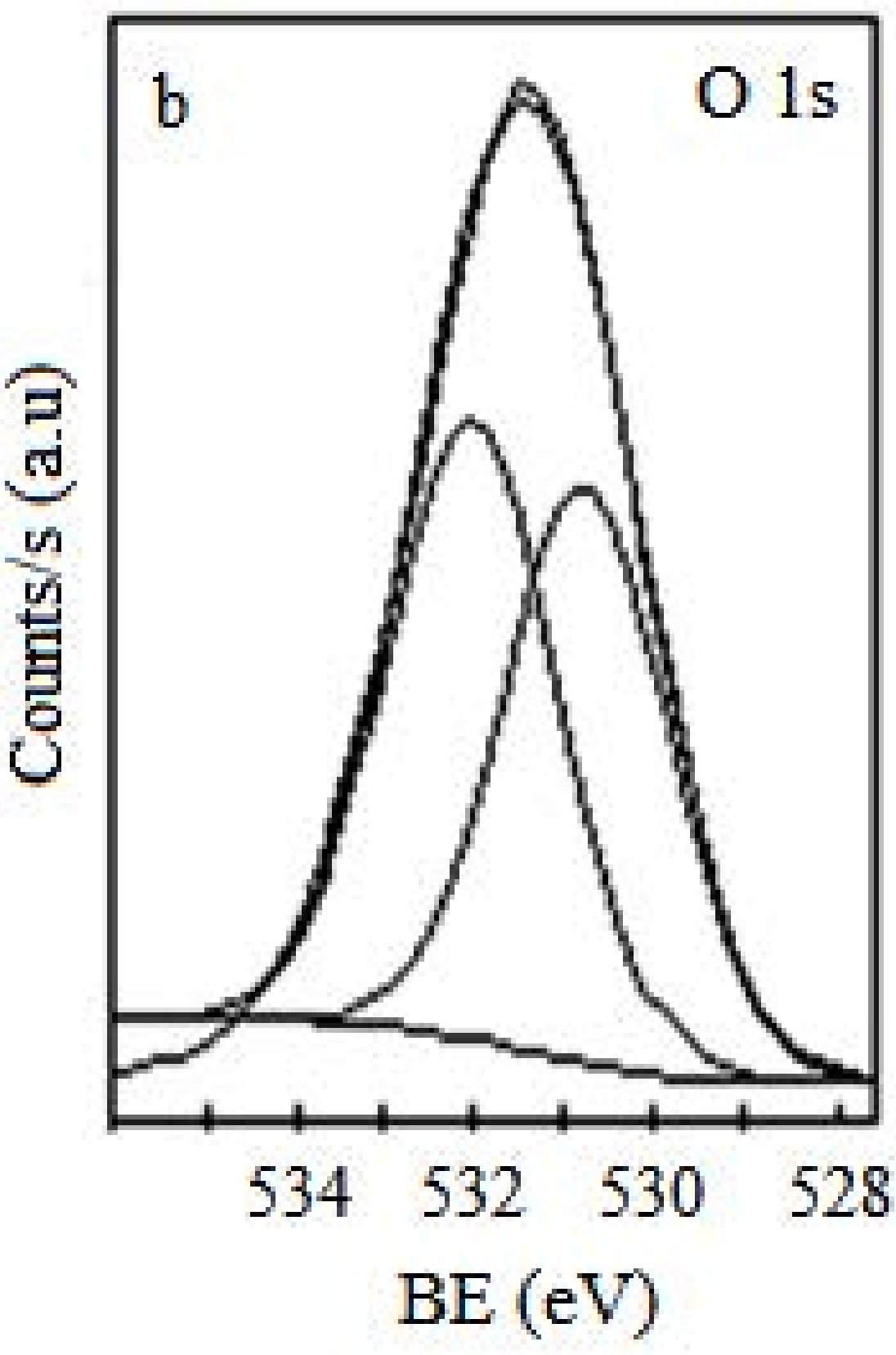
b
O 1s
Counts/s (a.u)
534
532
530
528
BE (eV)

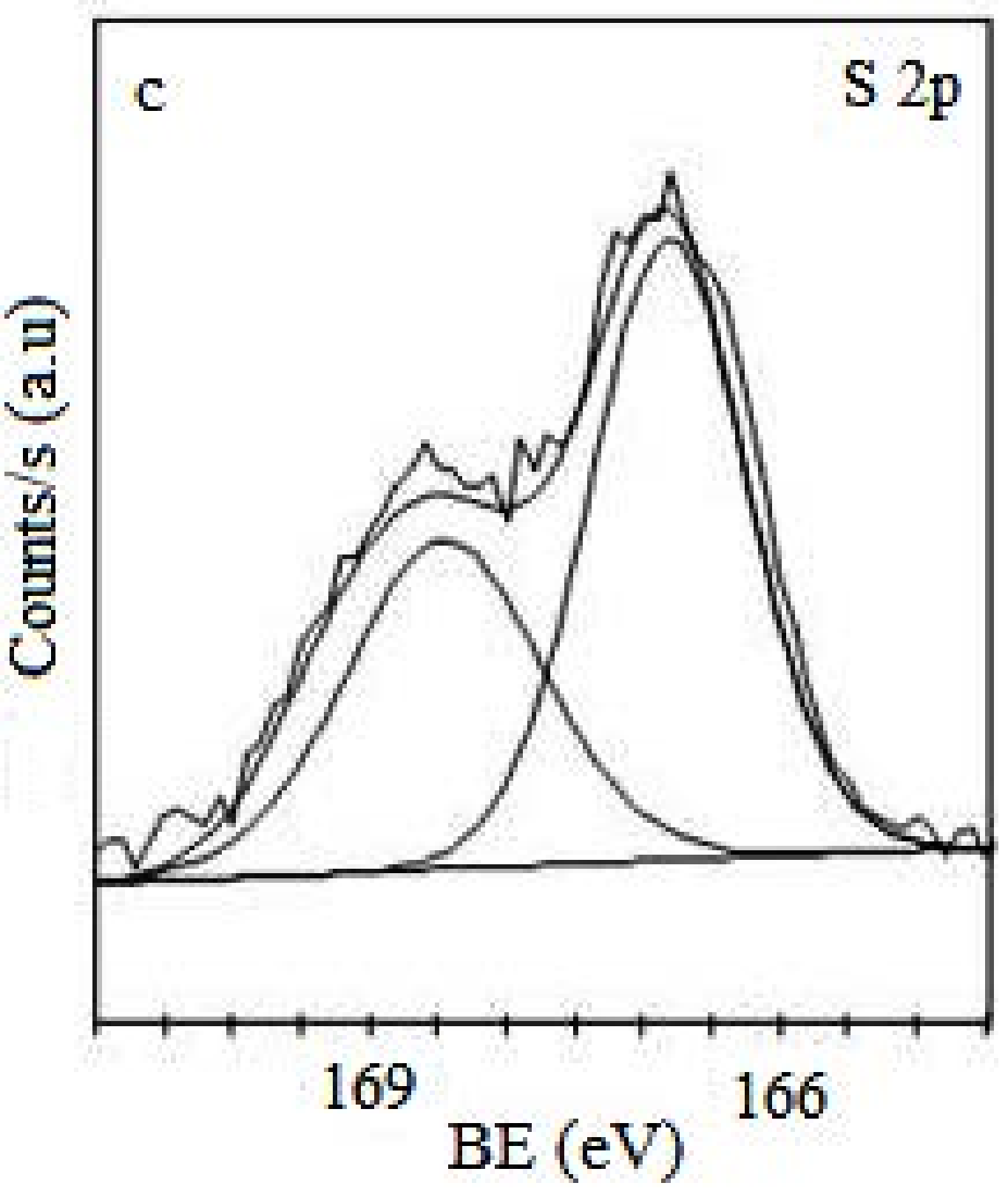
c
S 2p
Counts/s (a.u)
169
166
BE (eV)

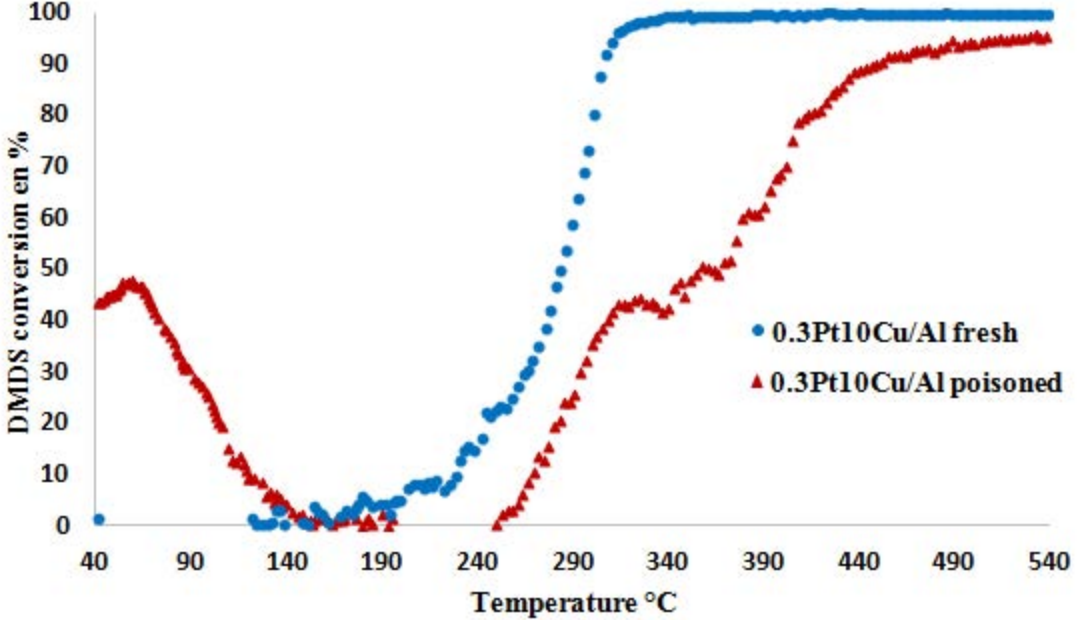
DMDS conversion en %
100
90
80
70
60
50
40
30
20
10
0
40
90
140
190
240
290
340
390
440
490
540
Temperature °C
0.3Pt10Cu/Al fresh
0.3Pt10Cu/Al poisoned

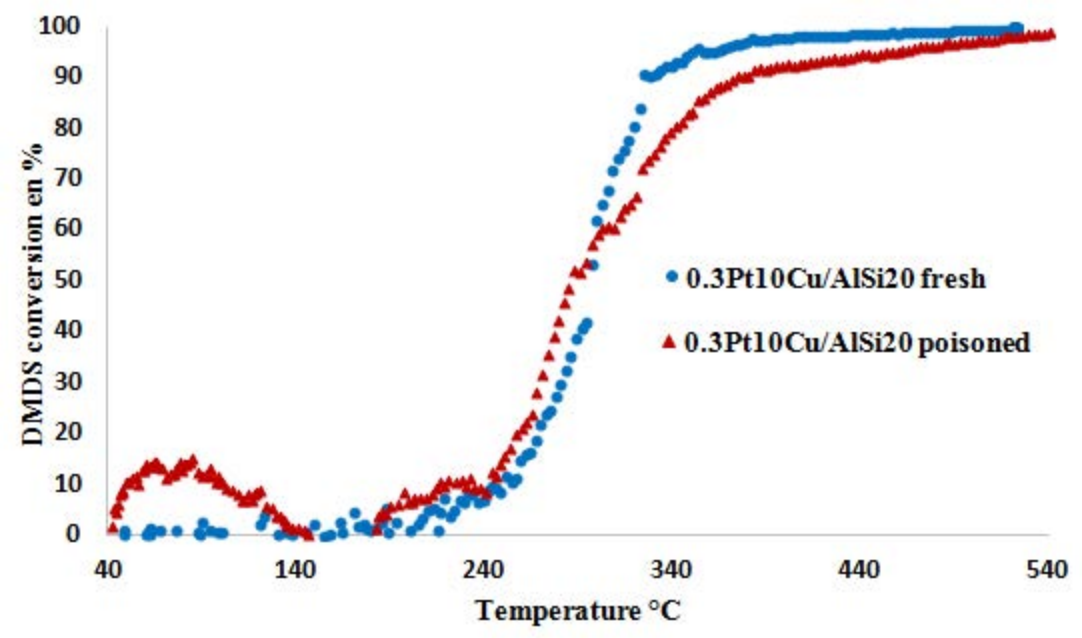
100
90
80
70
60
50
40
30
20
10
0
DMDS conversion en %
0.3Pt10Cu/AlSi20 fresh
0.3Pt10Cu/AlSi20 poisoned
40
140
240
340
440
540
Temperature °C

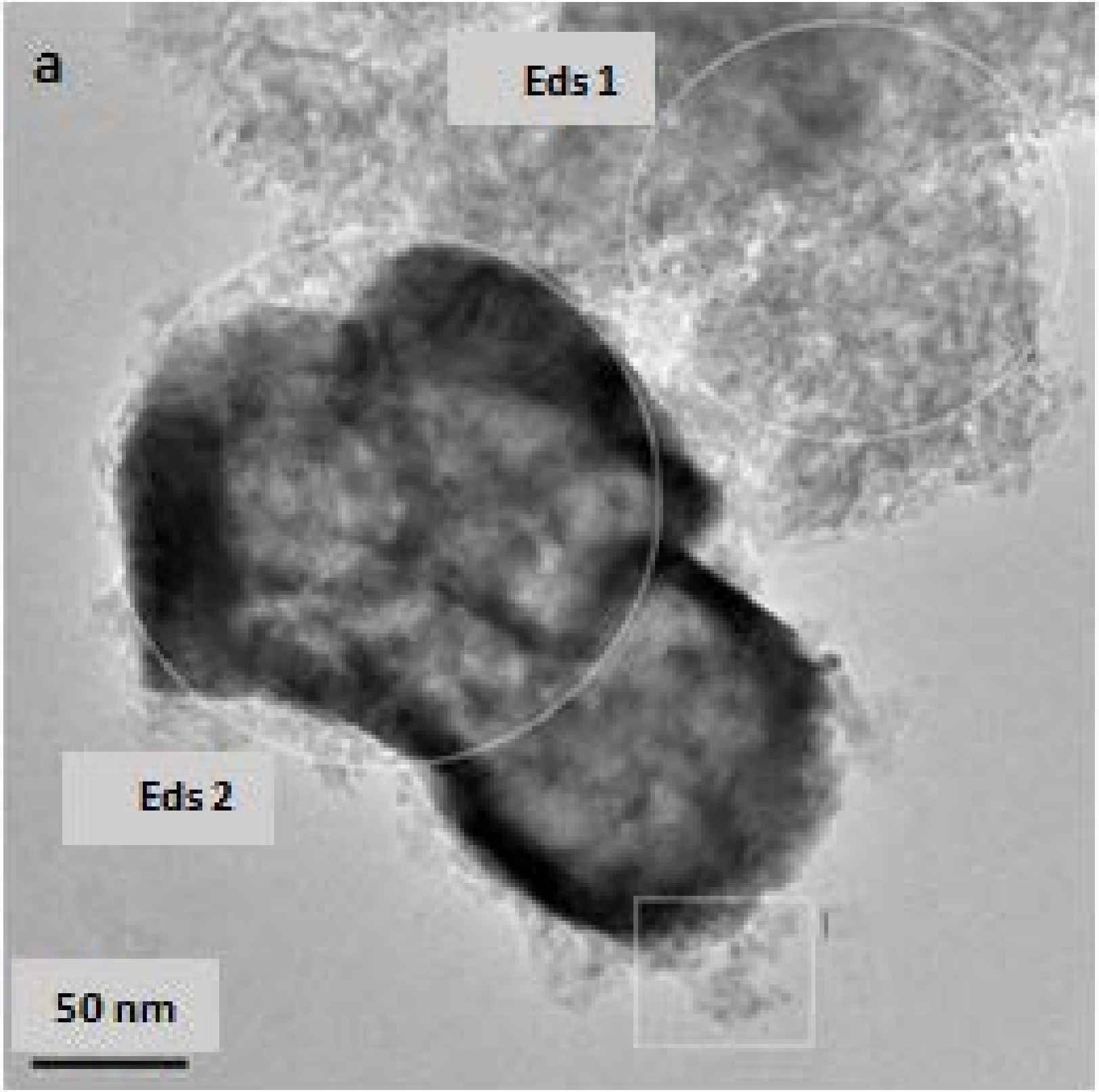
a
Eds 1
Eds 2
50 nm

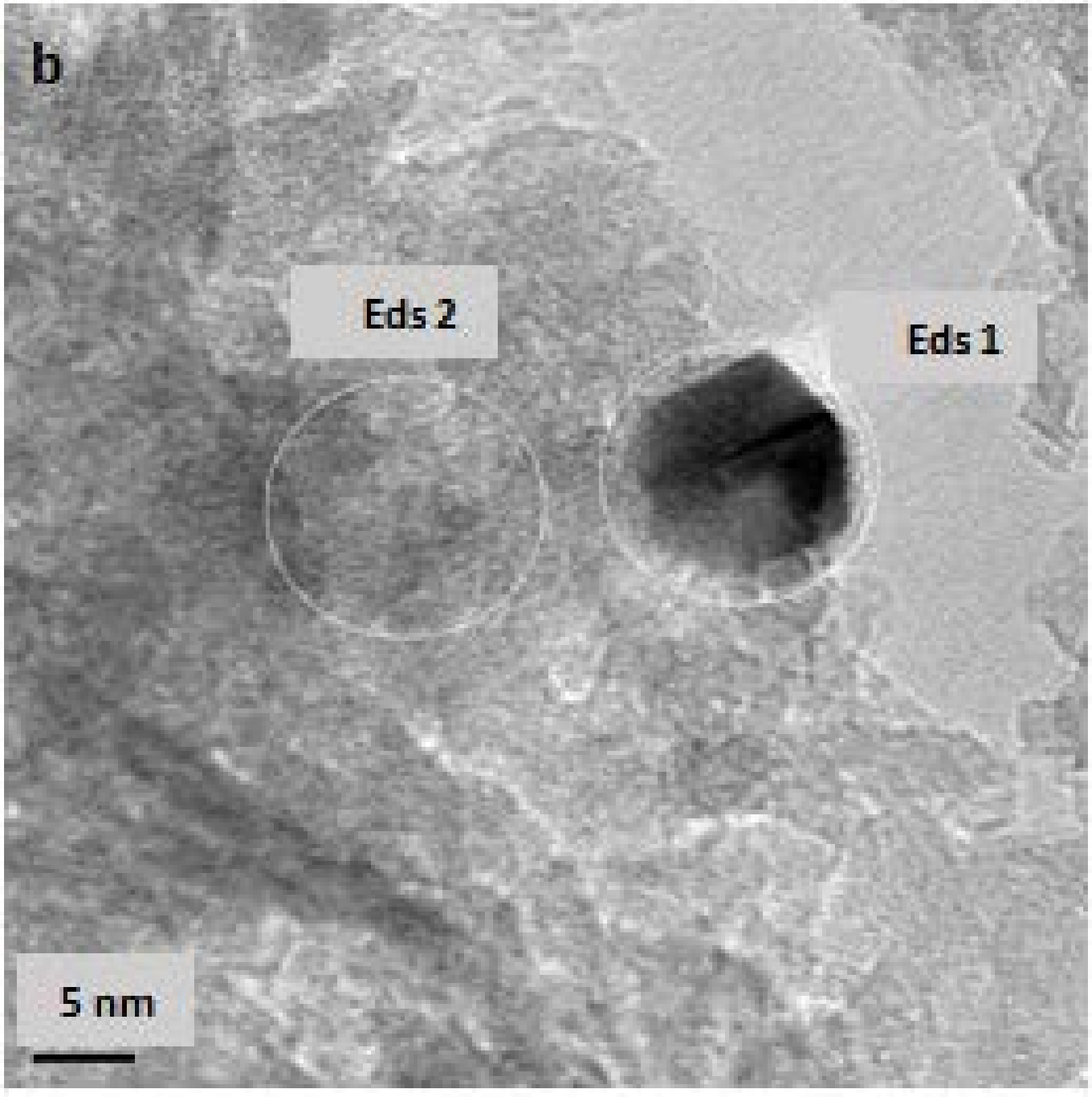
b
Eds 2
Eds 1
5 nm

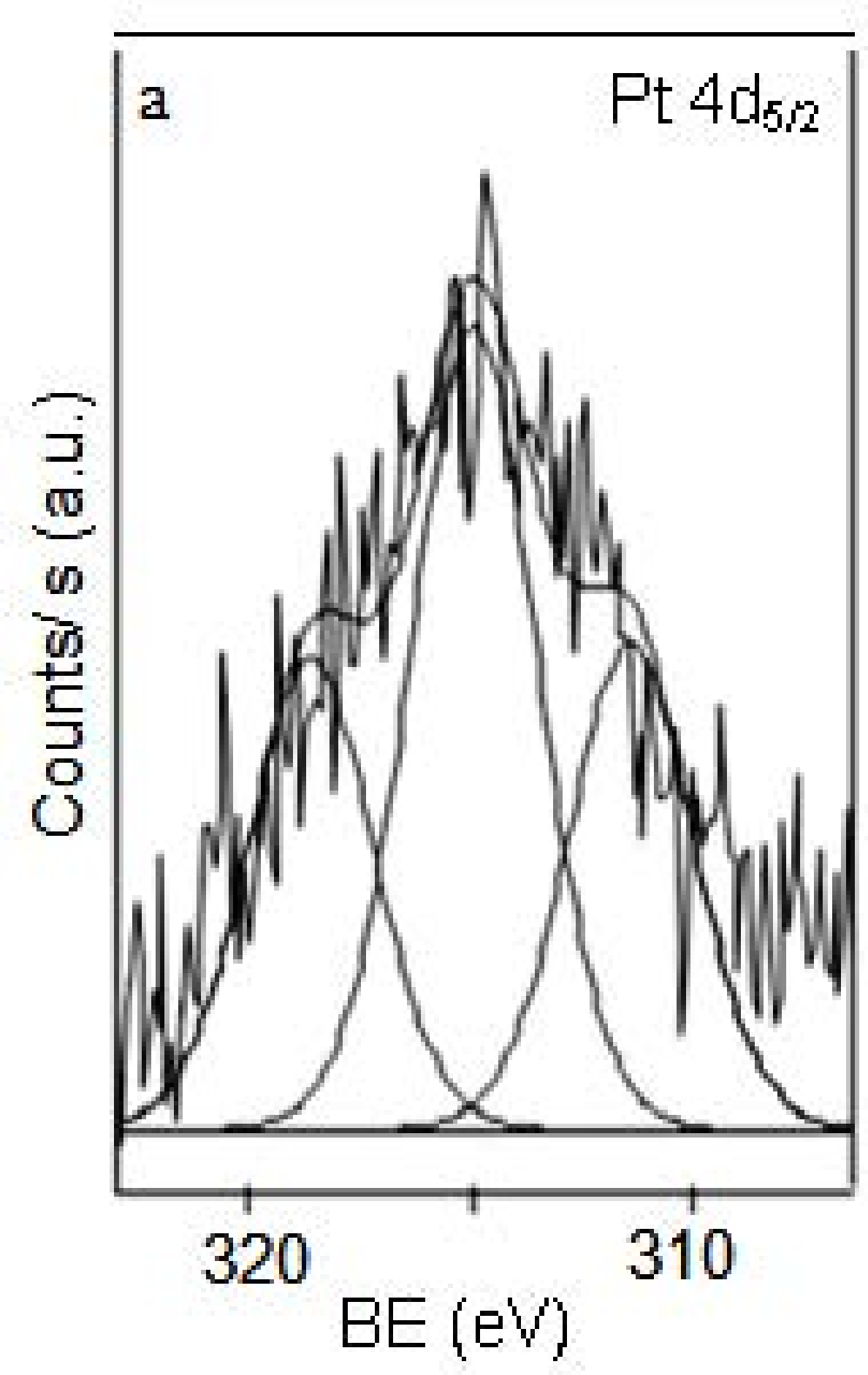
a
Pt 4d5/2
Counts/ s (a.u.)
320
310
BE (eV)

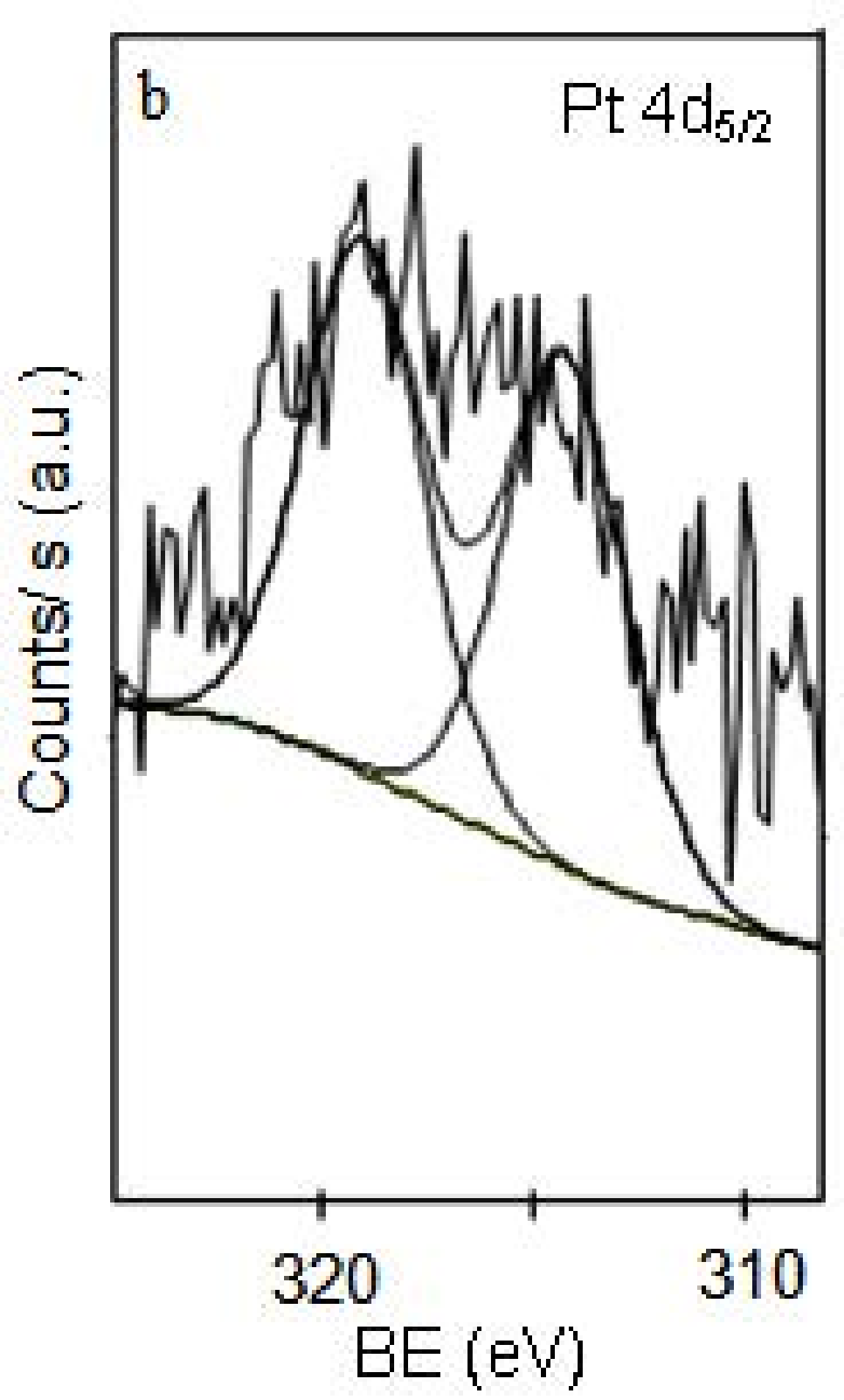
b
Pt 4d5/2
Counts/ s (a.u.)
320
310
BE (eV)

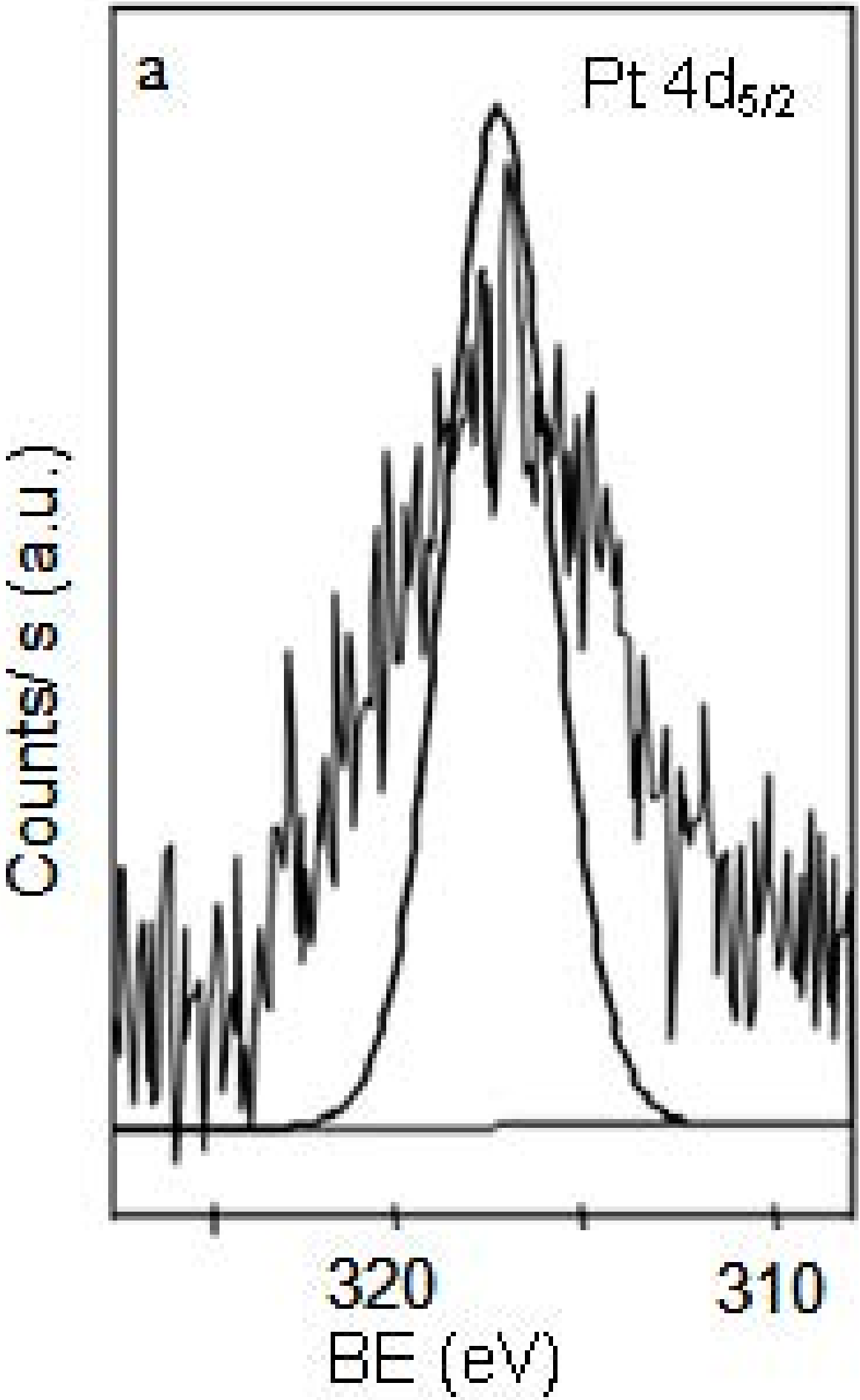
a
Pt 4d5/2
Counts/ s (a.u.)
320
310
BE (eV)

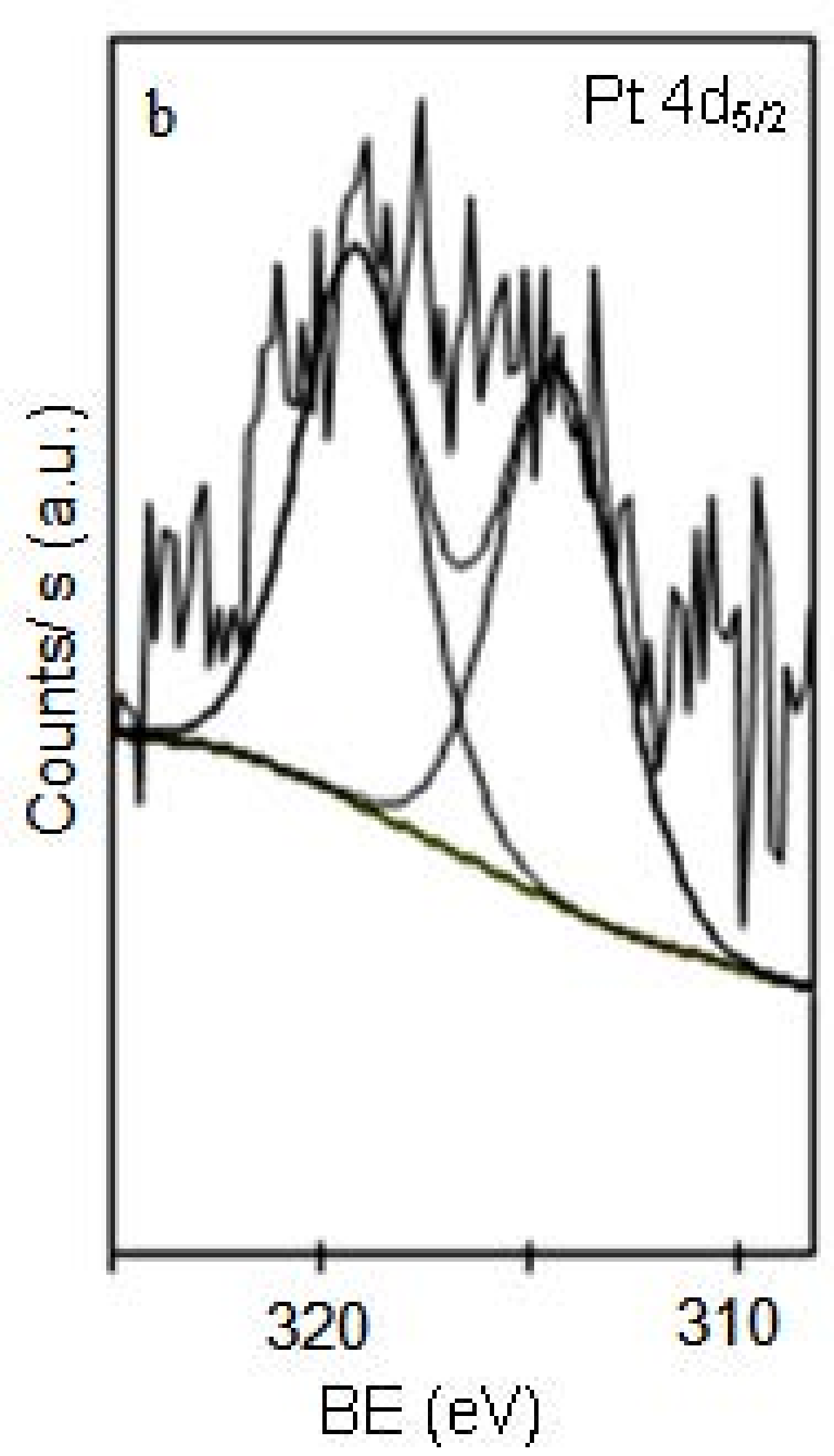
b
Pt 4d5/2
Counts/ s (a.u.)
320
310
BE (eV)

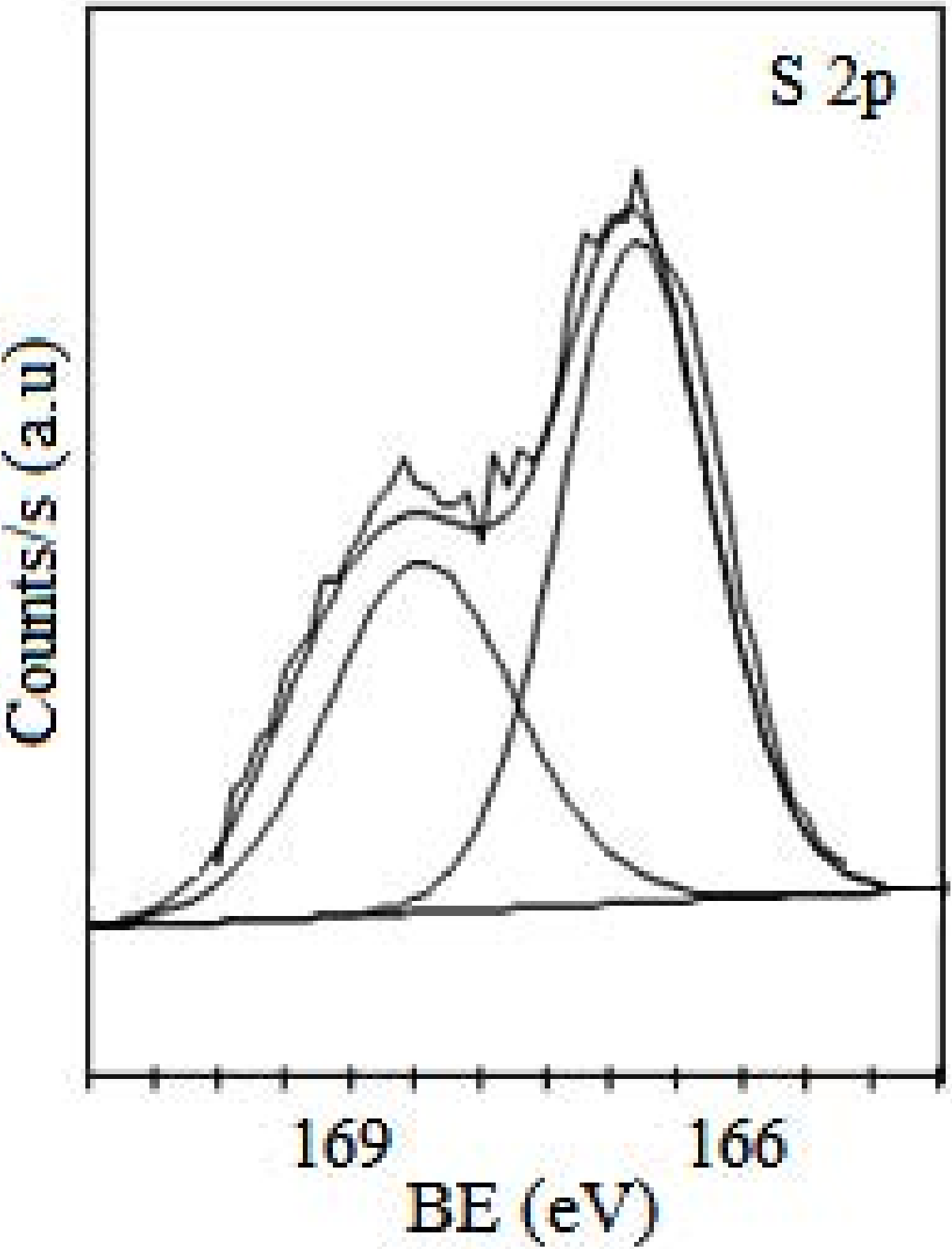
S 2p
Counts/s (a.u)
169
166
BE (eV)

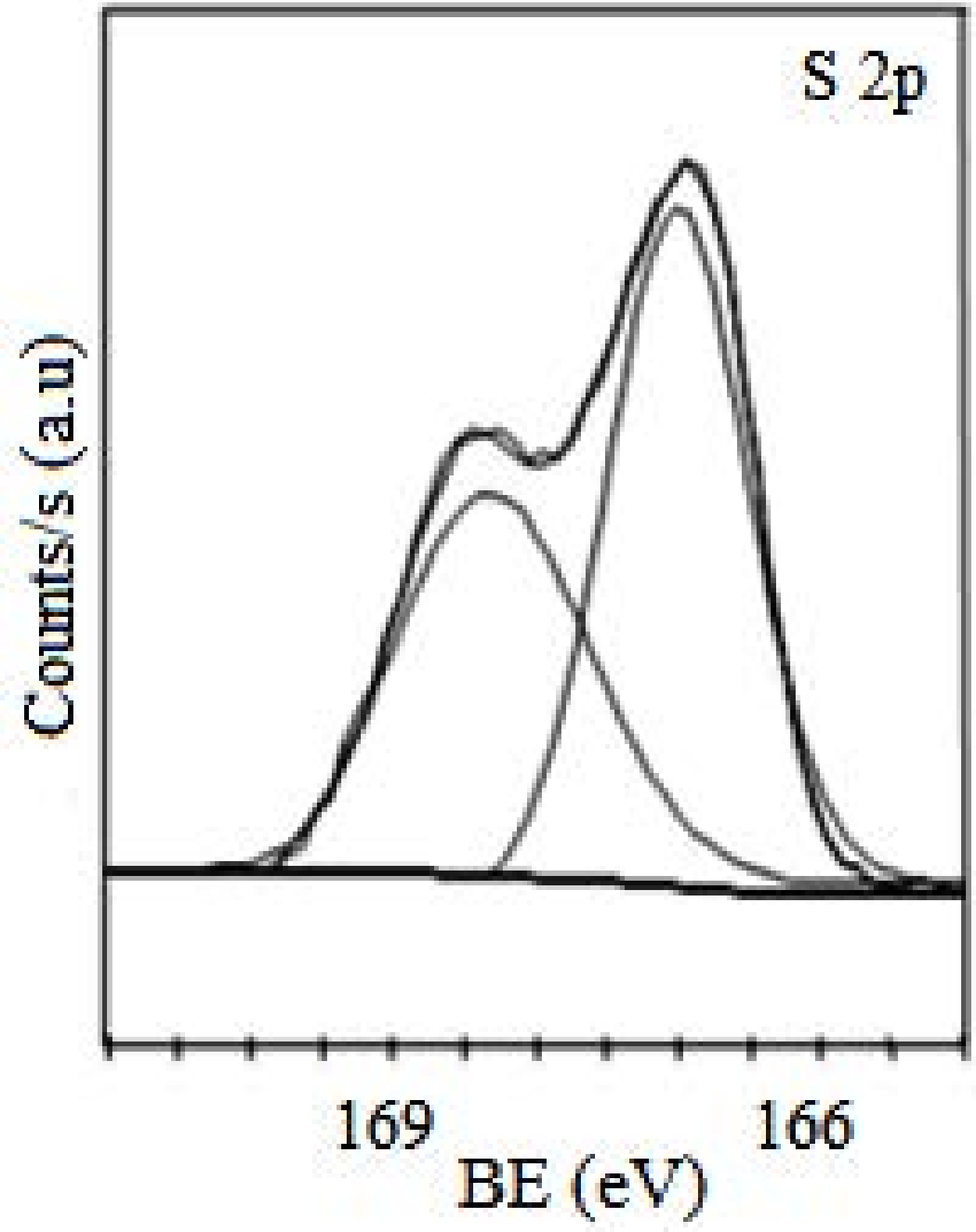
S 2p
Counts/s (a.u)
169
166
BE (eV)

Table 1. Light-off test temperatures; comparison of T_{50} and T_{90} in the oxidation of DMDS over fresh and used Pt/Al catalysts.

Catalyst	Treatment	T_{50} (°C)	T_{90} (°C)
Pt/Al	Fresh	375	425
	Used	404	454
	ΔT (°C)	29	29

Table 2. BET-BJH results of the fresh and used Pt/Al catalysts.

Catalysts	Specific surface area / $m^2.g^{-1}$	Total pore volume / $cm^3.g^{-1}$	Pore diameter / nm
Pt/Al fresh	190	0.44	9
Pt/Al used	10	0.01	5

Table 3. $T_{melting}$, T_{Tamman} and $T_{Hüttig}$ values (K) of metals and their compounds, relevant for heterogeneous catalysis [48].

compound	$T_{melting}$ (°C)	T_{Tamman} (°C)	$T_{Hüttig}$ (°C)
Pt	2028	1014	608
PtO	823	412	247
PtO_2	723	362	217
CuO	1599	800	480
Al_2O_3	2318	1159	695

Table 4. EDS analysis from different Pt particles on the surface of the used Pt/Al catalyst.

EDS analysis	O	Al	S	Pt	Total (Atom-%)
Eds 1 on Pt particle	46.2	38.8	4.2	10.8	100
Eds 2 on support	60.4	37.1	2.4	0.1	100

Table 5. Atomic ratios of the fresh and used Pt/Al catalysts by XPS.

Catalysts	Al/catalyst	Pt/catalyst	S/Al
Fresh	18	0.02	-
Used	10	0.02	0.6

Table 6. Light-off test temperatures comparison (T_{50} and T_{90}) in the oxidation of DMDS over fresh, used and poisoned Pt/Al catalysts.

Catalyst	Treatment	T_{50} (°C)	T_{90} (°C)
Pt/Al	Fresh	375	425
	Used	404	454
	poisoned	392	440

Table 7. Results of BET-BJH of the fresh, used and poisoned Pt/Al catalysts.

Catalysts	Specific surface area / m^2g^{-1}	Total pore volume / cm^3g^{-1}	Pore diameter / nm
Pt/Al, fresh	190	0.44	9
Pt/Al, used (2 months)	10	0.01	5
Pt/Al, poisoned (5 h)	90	0.24	11

Table 8. EDS measurements for different Pt particles on the surface of the poisoned Pt/Al catalyst.

EDS analysis	O	Al	S	Pt	Total (Atom-%)
Eds 1on Pt particle	59.39	32.76	1.58	6.27	100
Eds 2 on support	63.95	36.01	0.02	0.01	100

Table 9. Atomic ratios of fresh, used and poisoned Pt/Al catalysts by XPS

Pt/Al	Al/catalyst	Pt/catalyst	Pt/Al	S/Al
Fresh	18	0.02	0.001	-
Used	10	0.02	0.002	0.6
Poisoned	17	0.02	0.001	0.2

Table 10. T_{90} and T_{50} of DMDS oxidation over fresh and poisoned 0.3Pt10Cu/Al and 0.3Pt10Cu/$AlSi_{20}$ catalysts.

Catalysts	0.3Pt10Cu/Al	0.3Pt10Cu/$AlSi_{20}$
T_{90} of fresh (°C)	310	320
T_{50} of fresh (°C)	285	300
T_{90} of poisoned(°C)	400	365
T_{50} of poisoned(°C)	330	285

Table 11. Results of BET-BJH of fresh and poisoned 0.3Pt10Cu/Al and 0.3Pt10Cu/$AlSi_{20}$ catalysts.

Catalysts	Specific surface area / m^2g^{-1}	Total pore volume / cm^3g^{-1}	Pore diameter / nm
0.3Pt10Cu/Al, fresh	220	0.4	7
0.3Pt10Cu/Al, poisoned	130	0.3	7
0.3Pt10Cu/$AlSi_{20}$, fresh	290	0.6	8
0.3Pt10Cu/$AlSi_{20}$,poisoned	180	0.3	7

Table 12. EDS measurements for different Pt particles on the surface of the poisoned 0.3Pt10Cu/Al and 0.3Pt10Cu/$AlSi_{20}$ catalyst.

EDS analysis	O	Al	Si	S	Pt	Cu	Total (Atom-%)
Eds 1-b on Pt particle	45.58	32.86	2.04	0.00	15	4.51	100
Eds 2-b on support	58.14	34.75	3.78	0.42	0.07	2.84	100
Eds 2-a on Pt	47.10	11.98	--	3.09	5.12	32.7	100
Eds 1-a on support	59.25	37.09	--	0.78	0.00	2.88	100

Table 13. Atomic ratios on the surface of the fresh and poisoned 0.3Pt10Cu/Al and 0.3Pt10Cu/$AlSi_{20}$ catalysts according to XPS analysis.

0.3Pt10Cu/Al	Cu/Al	Pt/Al	S/Al
0.3Pt10Cu/Al, fresh	0.13	0.0033	--
0.3Pt10Cu/Al, poisoned	0.09	0.0022	0.1
0.3Pt10Cu/$AlSi_{20}$, fresh	0.16	0.004	--
0.3Pt10Cu/$AlSi_{20}$, poisoned	0.12	0.0035	0.08